Preferred citation: J-C. Roux. Pulp Treatment Processes. In **The science of papermaking**, *Trans. of the XIIth Fund. Res. Symp. Oxford, 2001*, (C.F. Baker, ed.), pp 19–80, FRC, Manchester, 2018. DOI: 10.15376/frc.2001.1.19.

STOCK PREPARATION PART 1 – PULP TREATMENT PROCESSES

Jean-Claude Roux

Laboratoire de Génie des Procédés Papetiers
UMR 5518 au CNRS/INPG/CTP/EFPG
Ecole Française de Papeterie et des Industries Graphiques
BP 65 – 38402 Saint-Martin d'Hères Cedex – FRANCE
Jean-Claude.Roux@efpg.inpg.fr

ABSTRACT

The re-pulping, refining and hot dispersing processes are considered in this first part "Pulp Treatment Processes" of the review paper about "Stock Preparation", which focuses on the process engineering aspects of the unit operations used in the production of virgin and recycled pulps. Chemical and physical-chemical aspects are beyond the scope of this paper, as are pulp dilution, transport and storage.

The pulp treatment processes refer to the unit operations aiming at altering and/or upgrading the fibrous raw material and associated solid materials and contraries (inks and various contaminants). They include re-pulping or disintegration, refining or beating, hot dispersing and mixing. Pulp disintegration has curiously never been of great interest to the paper science community, and hence remains an area of investigation where quite substantial benefits could be gained through reductions in energy consumption. Some new approaches will be presented that get round the difficult concept of pulp apparent viscosity, which is really an aspect of rheology. One of the main operations in stock preparation is obviously pulp. While the effects of refining on fibres have been extensively studied in the past, its engineering parameters

have not. For example, we do not yet know how to extrapolate refining results from the pilot to the industrial scale. It is even difficult to compare the effects of conical and disc refiners on the same pulp. It seems that only an integrated approach can improve our understanding of this process; one such will be proposed, building on fundamental engineering principles.

Then, the paper goes on to consider hot dispersion, an important process step in the field of paper recycling and deinking, to complete the effects of pulping and/or refining in terms of ink detachment, alteration of contaminants and fibre conformability. Hot dispersion is generally combined with bleaching because of the high temperature, consistency and mixing effect.

INTRODUCTION

Stock preparation, in the broad sense of producing a fibre suspension in a suitable form for the paper machine from the various fibre resources, includes the manufacture of chemical pulps, high-yield pulps and non-wood pulps as well as the recycling of recovered papers. The mechanical processes used in these applications can be classified in two main groups, considered in the two parts of this review:

- Pulp treatment processes: pulping, refining and hot dispersing.
- Particle separation processes: screening, cleaning, flotation and washing.

Chemical processes and physical-chemical aspects are outside the scope of this paper, as are wood and water treatment, and pulp dilution, transport and storage. The pulp treatment processes considered in this first part are of concern in the various sectors of stock preparation.

In chemical pulp mills, high consistency refining is normally used for the production of unbleached pulps for packaging applications. In the manufacture of high-yield pulps, the second refining stage and the associated screening systems are key steps in achieving the necessary fibre development and shive removal.

The recent introduction of the Bivis extruder for processing non-wood fibres must be mentioned. Bivis extrusion is a mechanical pulping process, with a defibreing action lying between grinding and refining [1,2]. It also functions as both a high temperature short time reactor and a washer since chemicals can be added and dissolved material removed as the pulp moves along the two extrusion screws [3,4]. The Bivis process is used in the manufacture of printing and packaging papers from wood [1–4] and annual plants [5,6].

Re-pulping recovered paper is clearly an important process in recycling. The mechanical action in pulping has to be optimised so as to ensure adequate defibreing of the re-pulped paper, while avoiding excessive size reduction of the various contraries, which would reduce their removal in subsequent screening. In deinking, the process must also detach ink particles from the fibres, without excessive ink fragmentation, which would reduce removal in flotation. Hot dispersion is essential to detach residual inks for removal in a second deinking step. In packaging recycling, it is used to disperse residual contraries, especially hot melt glues and flakes, to sizes below the visible limit. However, current trends are to replace hot dispersing by fine screening, since the process, by not removing contaminants but only dispersing them, does not solve the problems of deposits on the paper machine.

Finally, refining is the key process in developing the strength properties of recycled papers, especially packaging grades, where it is usually performed on the separated long fibre fraction. Refining is also important in manufacturing deinking grades, especially in high quality graphic paper.

RE-PULPING/SLUSHING OPERATION

Technological description

Pulp disintegration is a three-way operation, consisting of agitation by bulk motion, mixing of the slurry and dispersion by reduction of the solid particle size. The objectives are to obtain a pumpable, homogeneous slurry and to separate contaminants, ink particles and fibres [7]. The equipment used depends mainly on the feeding process and on the furnish nature. In the case of a non integrated mill, the fibrous raw material is received as bales of 90–95% air dry sheets, which are re-pulped into a slush as needed. In the case of a pulp mill integrated with a paper mill, chemical, mechanical and/or recycled pulps may be pumped from storage chests in slush form (3–6%). In the case of a recycled fibre furnish, the pulp must be cleaned and screened to remove any undesirable materials which could damage stock preparation equipment. Then, broke, common to all types of paper mills, must also be slushed for reuse and blended into the furnish [8].

Depending on the consistency, various different technologies exist to perform pulp disintegration. This paper will not review all the technological solutions available in the market; certain typical solutions will be given as illustrative examples.

Figure 1 illustrates a classical pulper used in the low consistency range. It

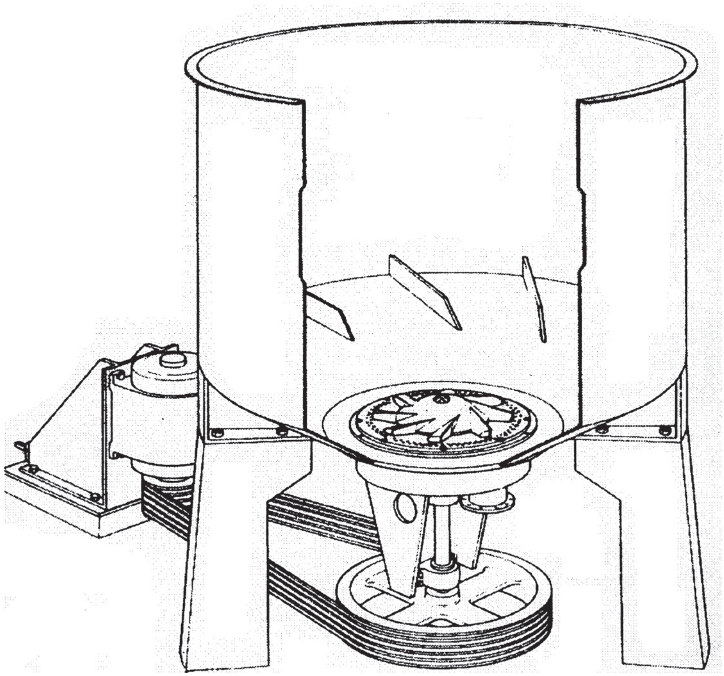

Figure 1 Classical pulper for low-consistency range [9].

consists of a tank with internal deflectors to promote efficient bulk motion, a rotor equipped with blades to induce shocks on contact with the pulp, and a perforated bed-plate to remove large size contaminants.

Figure 2 illustrates a pulper used where disintegration is performed in the medium consistency range. The main difference lies in the shape and the volume of the rotor; the helical vanes induce a motion to direct the pulp towards the agitated region near the rotor. Paraskevas [11] estimates that a pulper consumes from 5–15% of the total energy used in a paper mill. Despite this significant proportion, pulp disintegration has never stimulated any great interest in the paper science community. Reasons for this probably include the real difficulty of describing a three-way process dealing at the same time with agitation, mixing and dispersion of a pulp suspension; and the challenge of making direct measurements in a pulper. It seems that the technical literature very often reflects qualitative descriptions of the phenomena that occur during disintegration, following the work of Paraskevas [11] and Holik [12].

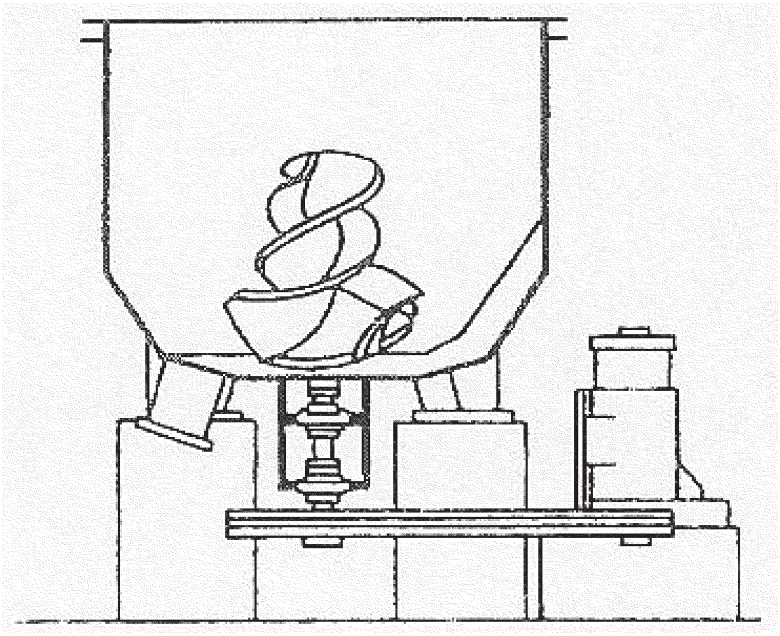

Figure 2 Medium consistency helical pulper [10].

According to the latter author, flakes can be broken down if certain forces are applied. These forces can be induced by clinging effects, "viscosity" effects and/or by acceleration effects. They contribute to the disintegration process through different criteria: their intensity, their application frequency and the minimum flake size reachable.

Physical description of the phenomena

Wagle *et al*. [13] gave insights into pulp floc dispersion mechanisms in a visual study performed in a turbulent Couette flow field. Even if the flocs are expected to be stronger than the ones on a paper machine (they were obtained in a laminar environment at the sedimentation concentration), this study reveals that two different mechanisms of disruption occur:

- a large scale stochastic phenomenon that involves deformation, breaking and fragmentation of the entire floc. This phenomenon depends on the structure of the floc, the imposed flow field and the duration of the stress.

Whenever the net tensile strength applied to the floc exceeds a minimum yield value, then the floc disrupts with a high rate process.

- a local small-scale erosion phenomenon which requires lower stresses and occurs over the entire surface of the floc.

These mechanisms can be linked in a first-order kinetic process to describe floc dispersion. This is of primary importance when one remembers that solid dispersion occurs simultaneously with agitation and mixing in the disintegration process.

Kinetics of disintegration

Only recently, Bennington [14] quantitatively described the kinetics of disintegration by considering the total area of the rotor in contact with the solid fibrous material. In this description, the interactions between fibres or flakes and rotor are responsible for pulp disintegration. If F stands for the flake content, the authors obtained:

$$\frac{dF}{dt} = k.F \tag{1}$$

where k is the first-order rate constant (negative value). Rewriting the previous equation as:

$$\frac{dF}{dC_R} = k'.F \tag{2}$$

where C_R is the fibre-rotor contact area given by the product of the volumetric concentration C_v and the area swept out by the rotor:

$$C_R = C_v.B.N.G.t \tag{3}$$

where N is the rotation speed of the rotor, B the number of rotor vanes, and G the surface area a single vane sweeps out during one revolution and t is the time. This model was validated for a single helical rotor, using varying rotor speeds and suspension consistencies and for three different furnishes. Figure 3, where the flake content is plotted versus the fibre-rotor contact area, illustrates this. All the consistencies are located on the same master curve for a given fibrous raw material.

The experimental results were in accordance with the model obtained by the integration of the differential equation (2):

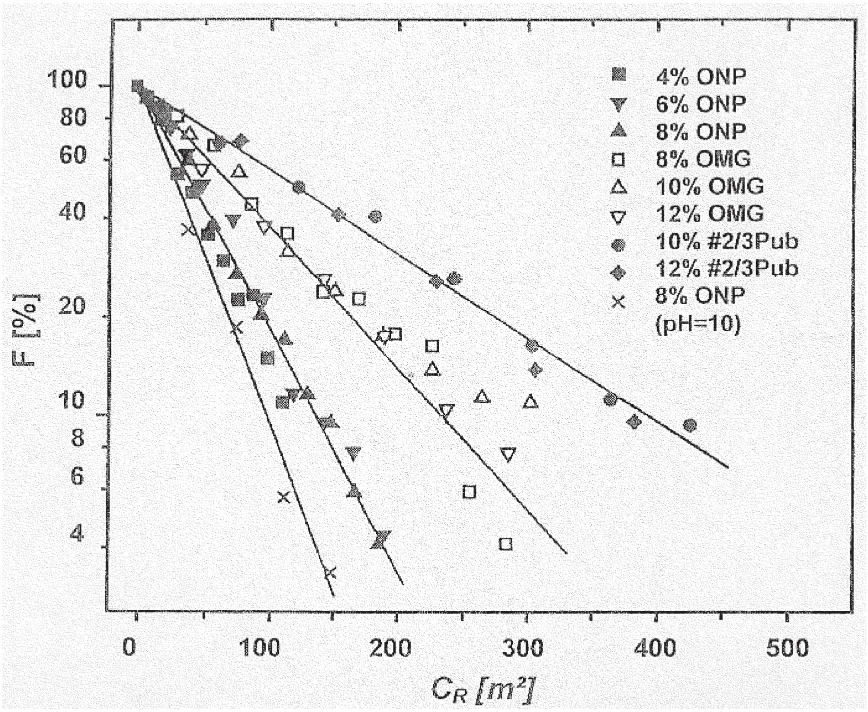

Figure 3 Flake content versus the fibre-rotor contact area C_R [14].

$$ln(F) = k'.C_R \tag{4}$$

In order to improve the knowledge and to generalise this approach taking into account all fibrous raw materials, the authors expected that the constant k' followed the Arrhenius equation used to describe chemical kinetics:

$$k' = k'_0, exp\left(-\frac{T_M}{K.F_R}\right) \tag{5}$$

where the material strength given by the wet tensile strength T_M was compared to the mechanical applied force F_R that can be evaluated using the net power P_n:

$$F_R = \frac{p_n}{\pi.D_m.N.B.H_c} \tag{6}$$

where D_m is the mean diameter of the rotor calculated by the mathematical average in the z-direction and H_c is the height of impeller in contact with suspension. With the help of both coefficients k'_0 and K, it is possible to successfully model the disintegration kinetics.

This approach is very interesting but concerns only the contact between the solid fibrous material and the rotor. It does not consider the disintegration effects that may occur from the fibre-fibre friction increasing with the mass consistency. Other attempts were investigated by Amaral *et al.* [15], Fabry *et al.* [16,17].

First attempt

The kinetics of the disintegration process can be assessed, for example, by counting the number of flakes per mass N of dry material, on sheet samples made with pulp at varying times during the operation. If the pulp is too strong to be disintegrated (wet strength materials), a number of indestructible flakes, N_∞, remains. So, one assumes that the number of flakes that are disintegrated per second is proportional to the remaining flakes that can be potentially processed and to the net power dissipated per volume of pulp suspension:

$$dN(t) = -b.[N(t) - N_\infty].\Phi_s.dt \tag{7}$$

where $N(t)$ is the number of counted flakes per mass at time t and Φ_s is the net power consumed per volume. This last differential equation may be integrated in a general sense and becomes:

$$N(t) - N_\infty = (N_0 - N_\infty).exp(-b.\int_0^i \Phi_s(t').dt') \tag{8}$$

The integral term is a key-factor in understanding the disintegration process; it defines the cumulative energy consumed per volume of pulp suspension. It is easier to consider that the net power per volume of pulp suspension is a constant value even if this assumption is not entirely true at the beginning of the process, where fluctuations have high amplitude (30% reported by Bennington and Fabry). With this simplified assumption, one obtains a first-order kinetic law compatible with the previous analysis:

$$N(t) - N_\infty = (N_0 - N_\infty).exp(-b.\Phi_s.t) \tag{9}$$

where the product $b.\Phi_s$ can be identified as the first-order rate constant k. This experimental law is validated for bleached Kraft eucalyptus and softwood pulps in a laboratory pulper where the volume is 4.5 dm^3, and for different times of water impregnation (0.5 h and 1 h), in the low consistency range (between 3% to 4.5%).

Table 1 illustrates the results obtained in these conditions.

Table 1 Determination of constants for the data of Amaral *et al.* [15].

Fibrous raw material	*Mass consistency x %*	0.5 h			1 h		
		Φ $10^5 J.m^{-3}.s^{-1}$	b $10^{-8}.J^{-1}.m^3$	k $10^{-3}s^{-1}$	Φ $10^5 J.m^{-3}.s^{-1}$	b $10^{-8} J^{-1}.m^3$	k $10^{-3}s^{-1}$
Eucalyptus	3.0	1.08	8.98	9.70	1.06	9.89	10.5
	3.5	1.20	5.18	6.22	1.10	8.76	9.64
	4.0	1.11	3.11	3.45	1.09	4.70	5.12
	4.5	1.14	6.61	7.54	1.13	4.14	4.65
Softwood pine	4.0	1.34	10.4	14.0	1.35	6.28	8.46
	4.5	1.47	5.49	8.07	1.42	6.45	9.16

Second attempt

Let us consider that the process kinetic follows a law of evolution written with the flake content F instead of the number of flakes per mass N:

$$dF(t) = -k.(F - F_\infty).dt \tag{10}$$

and suppose that the first-order kinetic constant k results from the product of a sensitivity term (a) by an average shearing stress in the bulk suspension ($\bar{\tau}$):

$$k = a.\bar{\tau} \tag{11}$$

If one assumes that the net power dissipated per unit volume can be attributed to the dissipation caused by an equivalent fluid, Rayleigh's law can be applied:

$$\Phi_s = \frac{(\bar{\tau})^2}{\mu} \tag{12}$$

where μ is a so-called apparent viscosity in Pa.s. Some difficulties may arise since this concept is not very well known in pulp suspension rheology and furthermore has not yet achieved wide acceptance in the scientific community. It seems desirable to consider this term as a shear-factor that incorporates all the friction forces (even the friction solid-solid forces) in a viscous form [16,17]. Fabry *et al.* demonstrated that this shear-factor is a strongly increasing function of the mass consistency (denoted x), so it may be written for the bleached softwood and hardwood Kraft pulps at consistencies below 10% as:

$$\mu = \mu_w . exp(\beta . x) \tag{13}$$

where μ_w is the dynamic viscosity of water.

Putting all the equations together, the first-order rate constant k becomes:

$$k = a.[\mu_w . \Phi_s . exp(\beta . x)]^{0.50} \tag{14}$$

The sensitivity constant a is then supposed to be a decreasing function of the mass consistency x. The previous expression suggests looking for an exponential solution, so an assumption is made accordingly:

$$a = a_0 . exp(- \lambda . x) \tag{15}$$

Whenever a disintegration trial is performed on a given pulper, with a given rotor, known fibrous materials and running consistencies, the first-order rate constant can be evaluated from flake measurements and the net power consumed per volume is also an information available.

$$k = a_0 . [\mu_w . \Phi_s]^{0.50} . exp(\sigma . x) \tag{16}$$

where:

$$\sigma = \frac{\beta}{2} - \lambda \tag{17}$$

When varying the consistency for different trials, equation (16) can be rewritten in order to determine both numerical values of a_0 and σ from a plot of the first right-term versus the mass consistency:

$$ln\{k.[\mu_w . \Phi_s]^{-0.50}\} = ln(a_0) + \sigma . x \tag{18}$$

This methodology was successfully applied to integrate the already published data of Amaral *et al*. [15], Merrett [18] and Savolainen *et al*. [19]. The results are given in the following Tables (2–4).

Table 2 Determination of the first-order kinetic constant k from Amaral *et al*. [15].

Fibrous raw material	*Mass consistency x %*	0.5 h		1 h	
		k $10^{-3}s^{-1}$	$ln[k.(\mu_w.\Phi_S)^{-0.5}]$	k $10^{-3}s^{-1}$	$ln[k.(\mu_w.\Phi_S)^{-0.5}]$
Eucalyptus	3.0	9.70	–6.98	10.5	–6.89
	3.5	6.22	–7.47	9.64	–6.99
	4.0	3.45	–8.02	5.12	–7.62
	4.5	7.54	n.d.	4.65	–7.73
Softwood	4.0	14.0	–6.72	8.46	n.d.
pine	4.5	8.07	–7.31	9.16	–7.17

Table 3 Determination of the first-order kinetic constant k from Merrett [18].

Fibrous raw material	*Temp. °C*	*pH*	*Mass cons. %*	Φ_s 10^4 $J.m^{-3}.s^{-1}$	k 10^{-3} s^{-1}	I_∞ %	$ln[k.(\mu_w.\Phi_S)^{-0.5}]$
Mixed of	47	10.1	4.8	1.96 ± 0.08	3.03	0.4	–7.29
waste	48	10.1	12.7	3.33 ± 0.47	5.97	0.4	–6.87
papers	60	10.2	14.4	3.24 ± 0.33	6.93	0.4	–6.71
Wet	73	11.2	5.5	2.07 ± 0.16	0.42	n.d.	–9.29
strength	74	10.6	14.0	3.22 ± 0.04	0.80	n.d.	–8.87
boards	79	11.8	14.0	3.15 ± 0.09	1.10	n.d.	–8.54

Table 4 Determination of the first-order kinetic constant k from Savolainen *et al*. [19].

Fibrous raw material	*Mass consistency %*	Φ_s 10^4 $J.m^{-3}.s^{-1}$	k 10^{-3} s^{-1}	$ln[k.(\mu_w.\Phi_S)^{-0.5}]$
Box	3.5	2.0	1.04	–8.37
corrugated	7.0		1.31	–8.14
papers	8.5		1.57	–7.95
Calendered	3.5	2.0	12.3	–5.90
papers	7.0		12.4	–5.89
	10		14.3	–5.75

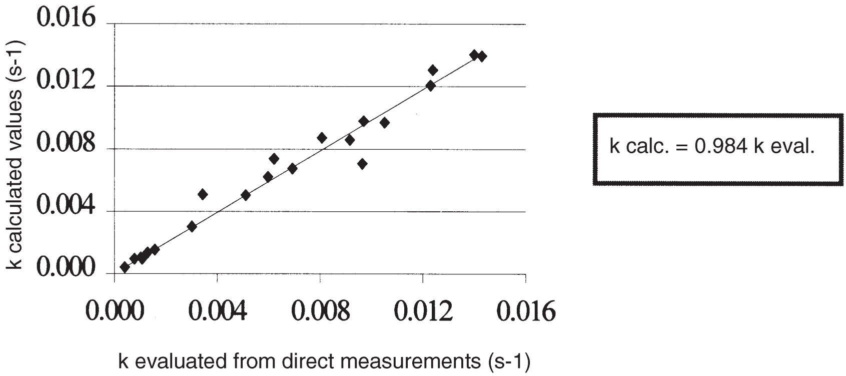

Figure 4 Comparison between the calculated and evaluated values of the kinetic constant for all the authors analysed.

The trials from Amaral *et al.* were performed in the low consistency range and negative values were obtained for σ. It reveals that the increase in the shear-factor with consistency, compared with the greatest possible decrease of the pulp sensitivity to disintegration, is not sufficient to increase the first-order constant rate of the process. As a consequence, this first-order rate constant k must always be a decreasing function of the mass consistency.

On the contrary, whenever trials have been performed in the medium consistency range, the σ coefficient has been found to be positive. This supports the well-established use of medium range consistency for pulp disintegration. Accounting for all the data available coming from different authors, the model proposed is as satisfactory as possible, as shown in Figure 4 which compares the kinetic constant evaluated from direct measurements and calculated according to the formula (16).

Table 5 Evaluation of the constants for kinetic modelling of pulp disintegration.

Authors	*Fibrous raw material*	a_0 $(Pa.s)^{-1}$	$1/a_0$ $Pa.s$	σ
Amaral *et al.*	Eucalyptus pulp	7.01×10^{-3}	143	−67
	Softwood pine pulp	8.08×10^{-2}	12.4	−105
Merrett	Mixed of waste papers	5.16×10^{-4}	1940	5.76
	Wet strength boards	6.31×10^{-5}	15,900	6.92
Savolainen *et al.*	Box corrugated papers	1.74×10^{-4}	5740	7.95
	Calendered papers	2.49×10^{-3}	403	2.26

If we compare the varying coefficients for all the pulps investigated, the term a_0^{-1} expresses an initial resistance of the fibrous raw material to disintegration. In Table 5, a classification of the propensity of varying pulps to be disintegrated is obtained: starting with the least resistance, we find: softwood Kraft pine pulps: then eucalyptus pulps: calendered papers: mixed waste papers: corrugated box papers; and, at last, wet strength boards.

Pulping: a key-operation for deinking [20]

In [14], Bennington *et al*. developed a model for the action of a helical pulper to study the effect of mechanical action on waste paper defibreing and ink detachment. Their model postulates that fibre/rotor interactions are responsible for defibreing. Knowledge of the area swept out by the rotor is necessary in this model, though its determination depends on measuring the height of the suspension in the pulper. Besides, with the introduction of chemicals, the underlying concept does not account for the flow modification that may occur. Previous work showed that differences of fragmentation and residual ink cannot be explained solely by physical-chemical phenomena [21]. The hypothesis of a mechanical action was then advanced. A rheological method was then used to estimate the shear-factor (generalisation of the viscosity) in a planetary mixer running as a pulper. This method was applied to 100% ONP (old newsprint papers) pulping to verify if mechanical action is correlated to ink fragmentation and ink removal by flotation.

Figure 5 illustrates the planetary mixer used. Whereas it is not yet used in the pulp and paper industry, it has found application as a pulper on a laboratory scale. With this type of mixer, defibreing is based on the application of heavy impact forces uniformly distributed between the impeller and the tank wall. The continuous change of impeller position (planetary motion) means that the motion of the pulp suspension differs from that in a classical pulper (see Figures 1 and 2). But this allows disintegration of 100% ONP at a consistency around 20% whereas a consistency of 9% is the limit for this furnish in a helical pulper. The high consistency increases friction between the fibres in the overall volume of the tank, not just around the impeller.

Rheological characterisation

The planetary mixer used in this study is a Hobart mixer. It has a volume of 10 dm^3 and the rotor speed can vary from 50 to 155 rpm. According to Metzner and Otto [22], the power required to rotate an impeller (with a rotation velocity N) in a mixing vessel can be expressed as a function of fluid properties (ρ density, μ dynamic viscosity) and of vessel geometry (d diameter

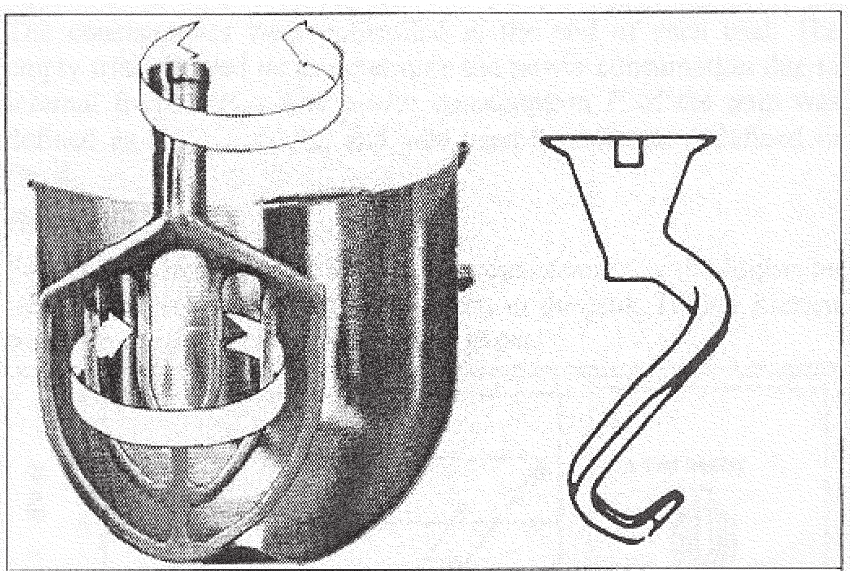

Figure 5 Hobart planetary mixer with flat beater on the left and hook impeller on the right.

of the rotor). The important ratios are the power number N_p first and the Reynolds number Re:

$$\frac{P_n}{\rho.N^3.d^5} = f\left(\frac{\rho.N.d^2}{\mu}, \text{vessel} - \text{geometry} - \text{factor}\right)$$

This analysis can be used to determine the characteristic curve of the impeller with Newtonian fluids (mixtures of water and glycerol solutions) where the viscosity is independent of the shear rate (and thus of the rotor speed). An example of this characteristic is represented in Figure 6 for the mixer with a hook impeller.

- At low Reynolds number below 200, the characteristic curve can be expressed by $N_p = K/Re$. The value of K depends on each type of impeller: 183 for the hook impeller and 371 for the flat beater. In the laminar area, it is possible to define an apparent viscosity accordingly:

$$\mu_{app} = \frac{P_n}{K.d^3.N^2} \tag{19}$$

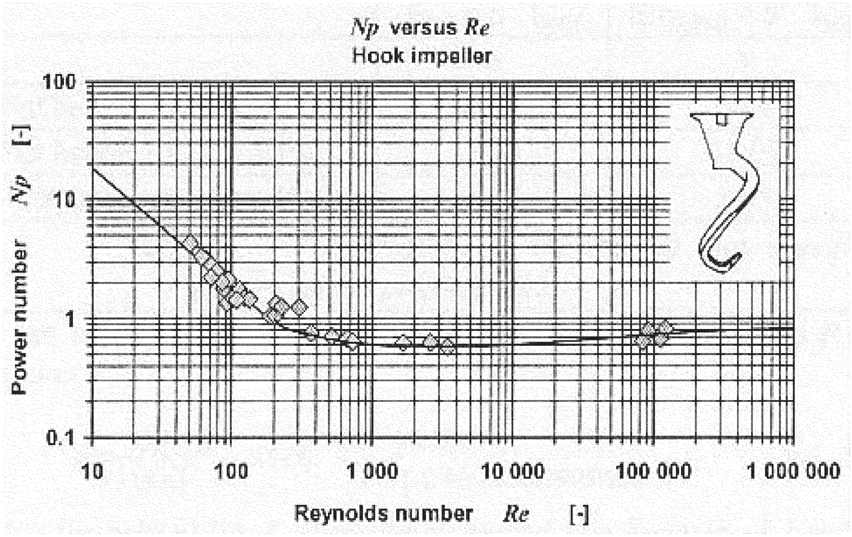

Figure 6 Characteristic curve of the Hobart mixer with a hook impeller.

- At high Reynolds number, the power number is independent of the Reynolds number.

A pulp is a non homogeneous and compressible medium, and, as the particles (fibres, flocs) can be deformed by shear, it is difficult and unrealistic to ascribe an apparent viscosity to a pulp suspension. This is especially true when the consistency is so high that its motion cannot be compared with that of a fluid. For these reasons, we prefer to generalise the apparent viscosity in a shear factor named λ to distinguish from the apparent viscosity. In this approach, we posit that the total amount of energy consumed is supposed to be consumed by friction of any kind. This overall friction is analogous to the liquid friction of an equivalent fluid which consumes the same power at the same rotor speed.

The results obtained with the planetary Hobart mixer are illustrated in Figure 7. The shear factor is an increasing function of the consistency. For a given consistency, the flat beater leads to a higher value of λ than the hook impeller. This may be due to higher contact area with the fibre and hence would be consistent with Bennington *et al*. [14] analysis. λ is a quantification of the overall friction phenomena that occur in the mixer: higher friction helps defibreing.

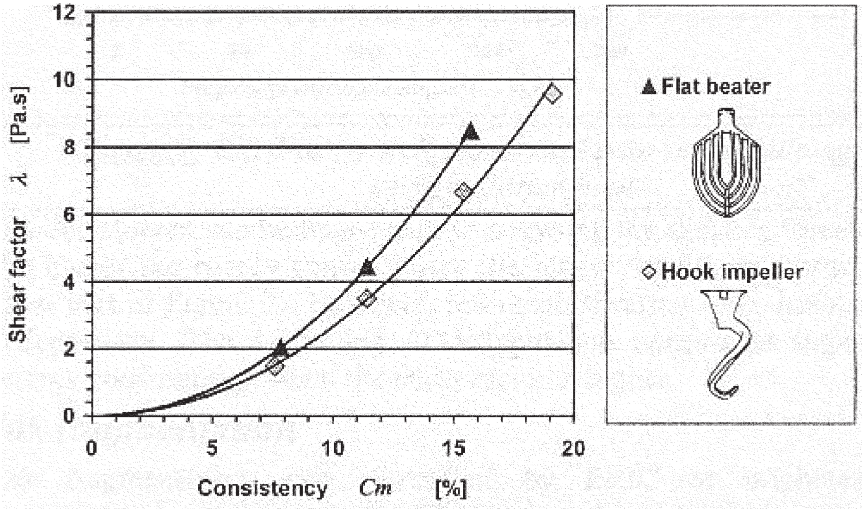

Figure 7 Shear factor as a function of consistency and impeller geometry.

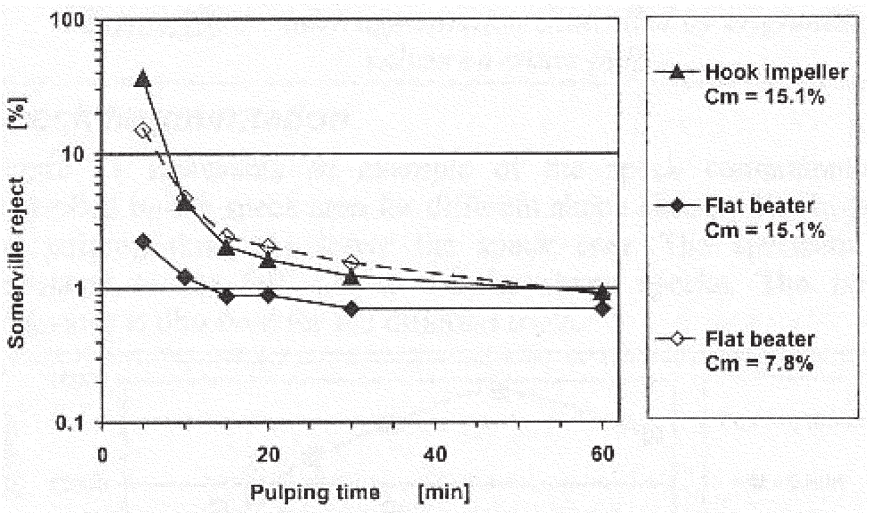

Figure 8 Defibreing of 100% ONP versus pulping time.

The defibreing degree was assessed by the flake content measured in a Somerville apparatus with slots of 8/100 mm width. The flake content is shown in Figure 8 versus pulping times, where it is seen that the flat beater leads to an increase in the defibreing kinetics. The effect of consistency is well known and has already been reported [11,12].

A master curve can be obtained if the flake content is plotted versus the energy consumption. This result is remarkable and reveals that this curve is independent of both the impeller type and the pulping consistency. Thus, the defibreing level of the pulp can be known if the energy consumption is measured: the higher the energy, the lower the flake content. This is illustrated in Figure 9.

Papermakers using recycled fibre are mainly concerned with the problem of the ink fragmentation that may occur in the defibreing stages. Brightness measurements were performed on the entire pulp and reveal that another master curve is obtained when plotting this brightness versus the pulping energy consumption. This curve, in Figure 10, is independent of the impeller type and of the consistency.

In order to demonstrate that the main physical quantity to assess defibreing is the energy consumption, Figure 11 illustrates the speck contamination versus the pulping energy consumption. Once again, a master curve is obtained whatever the impeller type and the consistency. The higher the

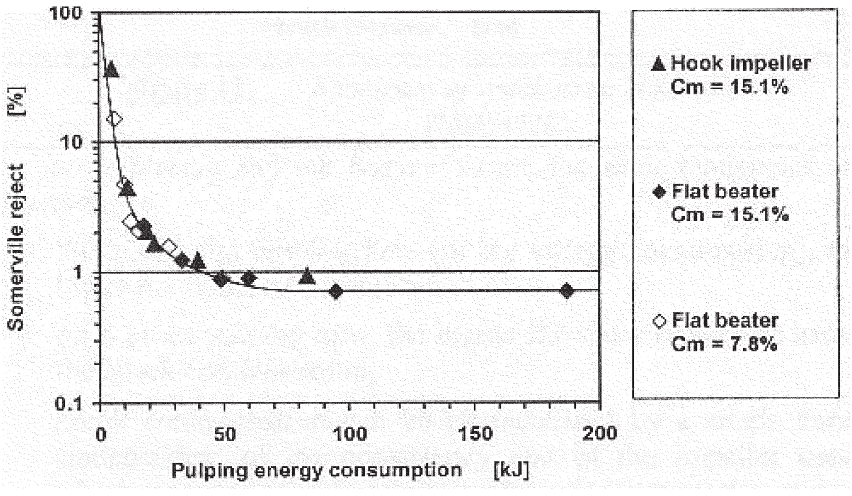

Figure 9 Defibreing versus pulping energy consumption.

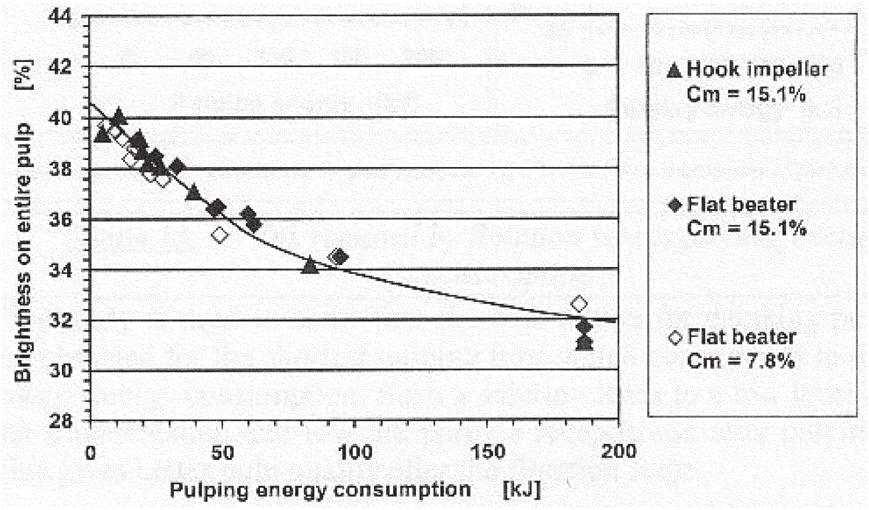

Figure 10 Ink fragmentation versus pulping energy consumption.

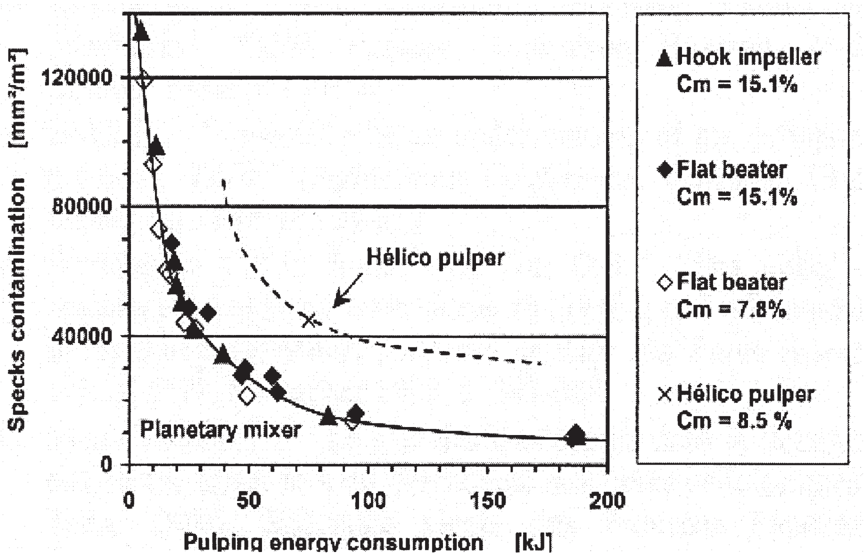

Figure 11 Speck contamination versus pulping energy consumption.

pulping energy consumption, the lower the speck contamination. The helical pulper is given as comparison.

In high consistency disintegration (8–20%), the energy consumed is given by the following expression:

$$E(t) = K.\lambda.N^2.d^3.t$$

This last expression gives prominence to two influences:

- a geometrical term related to the area swept out by the rotor in contact with fibre suspension in the effective shearing zone. These parameters (K, d) can be adjusted by the machinery suppliers;
- a rheological term, through the shear factor λ, related to an average shear during pulping. Adding chemicals such as soda may influence the shear factor and hence the resistance of the flakes to breaking down.

In order to obtain a good pulp quality in the disintegration stage, sufficient energy must be consumed, as was proved for the defibreing effects with the Somerville index and for speck contamination. However, overall pulp brightness shows an opposite tendency with increasing energy consumption, due to ink fragmentation. A solution may be obtained by reducing the pulping time and increasing the shear factor. In that case, the expected process gains are as follows: better pulp quality, higher productivity, energy saving and lower contaminant fragmentation.

REFINING/BEATING PROCESS

Technological description of the refining operation

Several excellent review papers [23,24,25] have already been devoted to the refining/beating process: a good example being that at the Ninth Symposium in Cambridge. The purpose of this new one is to identify some of the key quantities that play a role in the operation through a global, physical description of the phenomena.

Before recalling some generalities (more on the process itself than on its well known effects on fibres), a close look at Figure 12 shows that there is a rather wide choice in the technology of refining machines available on the market, from the old Hollander beater to the multi-disc. However, extrapolating refining results from pilot to industrial scale remains a key motive for addressing the operation of refining.

Fibres are refined or beaten in refining machines in the presence of water under both pressure and shearing action between surfaces in relative motion.

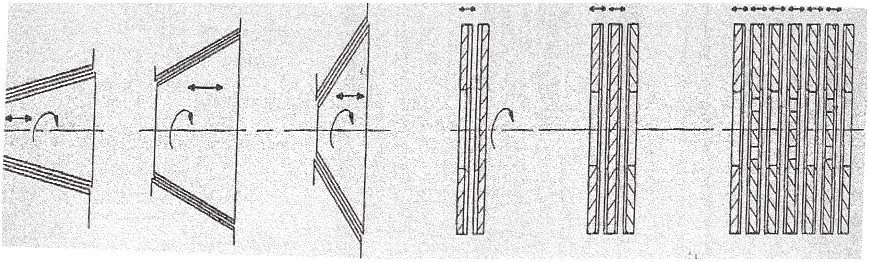

Figure 12 Different typical refining machines.

These surfaces may be fitted with bars on the bed-plate (or the stator) and the rotor, though these are not necessary to get refining action. However, most industrial refiners do have bars. Even in low-consistency refining (2–6%), the fibres do not remain single: they form flocs; and, as maximum shear rates may be very intense (in the order of magnitude of 5 to 6), these flocs re-disperse and re-form continuously.

A key quantity in all these machines is the gap clearance, the distance between the refining surfaces. This gap clearance must be sufficiently small to support the load. With water alone, it is impossible to form such a gap. It is only possible with pulp suspensions due to their load-carrying capacity. From these statements, it can be seen that the concepts of yield gap clearance (for refining effects to occur) and of loading force must be included in any full description of the refining/beating process. What can be learnt from the pulp flow in a disc-refiner for example? In the past, Fox *et al.* [26] investigated an experimental refiner at 1.1% consistency. Extrapolating their observations and analysis to low-consistency, the fibre-flocs are seen to be stapled against the leading edge of the stator bars, which are covered to between 50–70% of their width. However, it seems that the physics of the flow is very complicated and that understanding it fully is not easy. Centrifugal flows occur in the rotor grooves: centripetal reverse flows take place in the stator grooves, and intermixing flows between the two.

Many authors, e.g. Steenberg [27], have described the phenomena involved in the mechanics of refining; and it is essential to use their analysis as a starting point for any attempt at further quantification. Thus, in any refining machine, when the gap clearance is sufficiently small, the fibre-flocs consolidate when trapped between approaching tackle elements (relative motion and consolidation). Then when the surfaces overlap totally, a strong mechanical pressure is applied. Plastic deformation may occur at this stage. The shearing action is also intense since the tackle elements are moving and some fibre-flocs may be ruptured also. Then follows a relaxation of the mechanical pressure when water may be absorbed into the ruptured fibrils and fibres before turbulent agitation re-disperses the remnants into the general mass flow.

When it is said that the effects on fibres/flocs are better known, it does not mean that the probability of the occurrence of each effect is known [24]. According to Giertz [28], their probability distribution should follow a decreasing exponential function of the force intensity. As the intensity of the refining force increases, the following events are supposed to occur on the particles, with decreasing probability: elastic and/or visco-elastic deformation of fibres together with a frictional dissipation in water: intra-fibre H-bond breakage: unravelling of the cell wall: dislocations and delaminations; and finally, cutting and crushing of fibres. However, what are these forces involved in the process of refining? Can we explain the concept of refining intensity in terms of some realistic physical background?

In order to provide at least partial answers to these fundamental questions, we begin by studying the decomposition of normal forces or axial forces in single-disc refiners, with the help of a force balance, written for both large and narrow gap conditions [29]. Important results arise from this quantification of the process that agree with the findings of previous authors (e.g. Banks [30]). This leads to the concept of the shear-factor, already applied to characterize the disintegration process, and the purpose of this section dealing with beating is to exemplify its use in understanding refining. But before reaching this goal, the beating process needs to be more precisely defined in terms of engineering. Since several entire papers have pointed out the need to re-think the fundamentals of the refining process, we are proposing a new approach here. The shear factor is introduced to provide a physical understanding of the effective normal and tangential forces. These results are then compared to the engineering equation from Dalzell [31] and to the hydrodynamic modelling of Radoslavova *et al*. [32]. Interesting results are given in terms of a pressing process for disc refiners with the help of the shear factor [33]. Then, the refining kinetics are detailed. The last section ends up by giving some physical backgrounds to better define the classical refining intensity.

Physical description

Decomposition of normal forces in disc refiners

The demonstration can be performed on a single-disc refiner. When a pulp suspension flows through the small gap clearance between the refiner plates, tangential and normal forces are exerted on the plates themselves.

Leider and Nissan [34] described the mechanical behavior of a pulp suspension in a refiner as a solid or a liquid body, but it is more desirable to deal with the suspension as a two-phase material. An interesting starting point for the calculation of the elementary friction force over a small annulus between the radius ρ and $\rho + d\rho$ is:

$$dF_f(\rho,t) = f(t).\overline{P_m}(t).\xi.2\pi\rho.d\rho \qquad (20)$$

where $f(t)$ stands for an overall friction coefficient for the fibre suspension/metal bar combination. $\overline{P_m}(t)$ is the average mechanical pressure [35] exerted on the compressed fibrous pads in the inter-crossing areas of the bars of the refiner. ξ is the ratio of this inter-crossing area versus the global area, given by:

$$\xi = \frac{a_s a_r}{(a_s + b_s)(a_r + b_r)} \qquad (21)$$

where a and b are respectively the width of the bars and grooves, and the subscripts s, r stand for the stator and rotor disc respectively. In the same manner, the elementary normal force is given by the following:

$$dR_n(\rho,t) = \overline{P_m}(t).\xi.2\pi\rho.d\rho \qquad (22)$$

This force is exerted on the compressed fibre pads in all the confined zones (the intercrossing areas) in the gap clearance. An interesting and important point must be made that applies in Equations (20) and (22), under both refining and no-refining conditions. In order to find the overall force in the intercrossing areas, their integration must be performed over the annulus between the internal and external radii, ρ_i and ρ_e. Both the friction coefficient $f(t)$ and the average mechanical pressure $\overline{P_m}(t)$ are supposed to be uniform over the annulus to the first order. The integration of (20) and (22) leads to:

$$F_f(t) = f(t).\overline{P_m}(t).\xi.\pi(\rho_e^2 - \rho_i^2) \qquad (23)$$

and thus to the determination of the normal reaction force:

$$R_n(t) = \overline{P_m}(t).\xi.\pi(\rho_e^2 - \rho_i^2) = \frac{F_f(t)}{f(t)} \qquad (24)$$

If the gap clearance is large enough that no refining effect occurs on the pulp suspension (i.e. on the fibres), then equation (24) can be written:

$$R_n^0 = \overline{P_m^{\ 0}}.\xi.\pi(\rho_e^2 - \rho_i^2) \tag{25}$$

with the superscript ^{0} meaning no refining effect at all. It is likely that $\overline{P_m^{\ 0}}$ is a hydraulic pressure so it will be defined as $\overline{P_h}$. Hence, any measurement of $R_n^{\ 0}$, the reference normal reaction force, allows $\overline{P_h}$ to be determined. Based upon a series of trials, it was found that this pressure also applies in the grooves when the gap clearance is either small or large [36]. In either refining or no-refining situations, it is thus assumed that the pressure $\overline{P_h}$ is maintained in the grooves whatever the magnitude of the gap clearance, and that it is not a time-dependant quantity. Consequently, the normal reaction force R_n^0 is invariant and not affected by the state of refining of the pulp:

$$\frac{\partial R_n^0}{\partial t} = 0 \tag{26}$$

However, on the contrary the equivalent frictional force $F_f^{\ 0}$ may be affected by the refining state of the pulp according to:

$$F_f^{\ 0}(t) = f(t).R_n^0 \tag{27}$$

The previous remarks are of primary importance when it is desired to define the effective part of the normal reaction [37] and of the frictional force, since one reference may change with the time t:

$$\begin{cases} F_n^{eff}(t) = R_n(t) - R_n^0 \\ F_f^{eff}(t) = F_f(t) - F_f^0(t) \end{cases} \tag{28}$$

Taking into account Equations (24) and (25), under kinetic conditions the following expressions are obtained:

$$\begin{cases} F_n^{eff}(t) = (\overline{P_m}(t) - \overline{P_h}).\xi.\pi(\rho_e^2 - \rho_i^2) \\ F_f^{eff}(t) = f(t).F_n^{eff}(t) \end{cases} \tag{29}$$

Until now the only forces considered arise in the inter-crossing areas of bars. But any measurement of the normal compression force (or axial force) $F_n(t)$ has two contributions:

- the normal reaction force $R_n(t)$ in the inter-crossing area, and
- the additional force $\overline{P_h}.(1 - \xi).\pi\left(\rho_e^{\ 2} - \rho_i^2\right)$ in the complementary area.

Under refining conditions, this is written as follows:

$$F_n(t) = R_n(t) + \overline{P_h}.(1 - \xi).\pi(\rho_e^2 - \rho_i^2) \tag{30}$$

Under no-refining conditions, in the same manner:

$$F_n^{\,0} = R_n^0 + \overline{P_h}.(1 - \xi).\pi\left(\rho_e^2 - \rho_i^2\right) \tag{31}$$

As a consequence, the effective normal force is given by the expression:

$$F_n^{eff}(t) = F_n(t) - F_n^0 \tag{32}$$

Another way to write this is first to consider decomposing the acting normal force into two parts: one constant, and one varying with time:

$$F_n(t) = F_n^0 + F_n^{eff}(t) \tag{33}$$

From the previous analysis and with the help of the measurement of $F_n^{\,0}$ in no-refining conditions, the hydraulic pressure $\overline{P_h}$ can be determined:

$$\overline{P_h} = \frac{F_n^0}{\pi(\rho_e^2 - \rho_i^2)} \tag{34}$$

In the following paragraph, the formulae derived so far are applied to the refining of pulp suspensions. At this point, it is desirable to summarise the forces identified and how they can be measured.

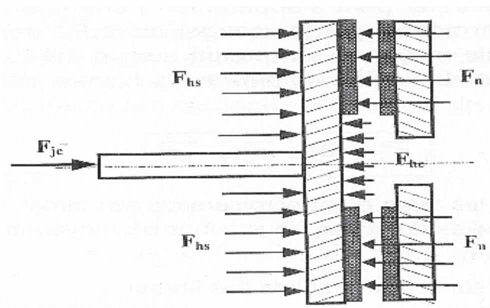

Figure 13 Single-disc refiner.

From the measurement of the axial force with a strain gauge device, the balance of forces allows the determination of the normal force:

$$F_n = F_{jc} + F_{hs} - F_{he} \tag{35}$$

Derivation of the net power

Different types of power can be defined in the refining process and it is possible to simply derive the net power from the previous analysis. The following demonstration of this derivation allows us to confirm the Banks formula, obtained in the early sixties [29]. The friction power consumed in a refiner can be determined by integration over the annulus of:

$$dP_f(\rho,t) = dF_f(\rho,t).2\pi\rho N \tag{36}$$

This then leads to:

$$P_f(t) = f(t).\overline{P_m}(t).\xi.\frac{4\pi^2(\rho_e^3 - \rho_i^3)}{3}.N \tag{37}$$

In the case of large gap clearance, the average mechanical pressure reverts to $\overline{P_h}$ already defined and explained:

$$P_f^0(t) = f(t).\overline{P_h}.\xi.\frac{4\pi^2(\rho_\varepsilon^3 - \rho_i^3)}{3}.N \tag{38}$$

It seems reasonable to admit that the net power may be calculated by the difference between the two previous powers:

$$P_{eff} = P_f(t) - P_f^0(t) \tag{39}$$

P_{eff} is written instead of $P_{eff}(t)$ to take account of the fact that a control system often imposes a constant refining power equal to a predefined setpoint value. Another detailed expression of the net power is given by:

$$P_{eff} = f(t).(\overline{P_m}(t) - \overline{P_h}).\xi.\frac{4\pi^2(\rho_e^3 - \rho_i^3)}{3}.N \tag{40}$$

If the relative mechanical pressure is replaced according to the effective force, then P_{eff} becomes:

$$P_{eff} = f(t).F_n^{eff}(t).2\pi.\frac{2\rho_e(1 - k^3)}{3(1 - k^2)}.N \tag{41}$$

with an effective radius $\bar{\rho}$ calculated from the ratio k of the internal to the external radius:

$$\bar{\rho} = \frac{2\rho_e(1-k^3)}{3(1-k^2)} \tag{42}$$

To summarize at this point, the measurements of both the normal compression force in loading $F_n(t)$ and no-loading $F_n^{\ 0}$ conditions allow the average mechanical pressure $\overline{P_m}(t)$ and the average hydraulic pressure $\overline{P_h}$ to be determined according to:

$$F_n^{\ 0} = \overline{P_h}.\pi(\rho_e^2 - \rho_i^2) \tag{43}$$

and:

$$F_n(t) = [\overline{P_h} + \xi.(\overline{P_m}(t) - \overline{P_h})].\pi(\rho_e^2 - \rho_i^2) \tag{44}$$

Then, from Equation (41), the friction coefficient can be obtained:

$$f(t) = \frac{3.P_{eff}}{(\overline{\mathrm{P}_{\mathrm{m}}}(t) - \overline{P_h}).\xi.4\pi^2\rho_e^3(1-k^3).N} \tag{45}$$

It is remarkable that Equation (41) gives legitimacy to the Banks formula empirically derived in the early sixties, though the author did not precisely define either the friction coefficient or the axial force acting on the shaft of a disc refiner. The previous derivations clarify the equation and give these definitions without any ambiguity.

The formulation between the net power and the shear factor

Previous published papers demonstrated that the shear factor Λ can be used to describe the flow of a pulp suspension in small shear gaps. Hence one point of departure could be to consider the pulp suspension as a homogeneous equivalent fluid, as was done by Leider and Nissan [34]. But it is more fruitful to generalize the pulp apparent viscosity μ_a by the shear factor Λ, keeping the complex reality of both the pulp suspension and the shear field in the gap clearance. The shear factor incorporates the geometrical parameters in addition to the fluid/suspension properties. In this case, the shear stress at the wall is given in terms of shear rate at the wall:

$$\tau_w(\rho,t) = \Lambda(\rho,t).\dot{\gamma}_w(\rho,t) \tag{46}$$

where the shear rate can be expressed:

$$\dot{\gamma}_w(\rho,t) = \frac{2\pi\rho N}{\bar{e}(t)} \tag{47}$$

$\bar{e}(t)$ stands for the mean gap clearance over the annulus. If the effective elementary frictional force is determined, one can obtain:

$$dF_f^{eff}(\rho,t) = \Lambda(\rho,t).\xi\frac{4\pi^2\rho^2 N}{\bar{e}(t)}.d\rho \tag{48}$$

A close examination of Equation (20) reveals that the shear factor $\Lambda(\rho,t)$ is inversely proportional to the radius ρ and the rotation speed N:

$$\Lambda(\rho,t) = \frac{C_1(t)}{2\pi\rho N} \tag{49}$$

In order to obtain an overall quantity to describe the shear behavior of a pulp fibrous suspension in disc refiners, the mean value of the shear factor Λ is calculated:

$$\overline{\Lambda}(t) = \frac{1}{\rho_e(1-k)}\int_{k.\rho_e}^{\rho_e}\Lambda(\rho,t).d\rho \tag{50}$$

Then, the integration of the effective elementary frictional force leads successively to:

$$F_f^{eff}(t) = \frac{C_1(t)}{\bar{e}(t)}.\xi.\pi\rho_e^2(1-k^2) \tag{51}$$

thence to the following equation with the mean shear factor $\overline{\Lambda}$:

$$F_f^{eff}(t) = \frac{\overline{\Lambda}(t)}{\bar{e}(t)}.\xi.\frac{2\pi^2\rho_e^3(1-k)(1-k^2)}{ln(1/k)}.N \tag{52}$$

If a refining trial is performed keeping constant the net power, P_{eff}, combining Equations (29), (41) and (42) with Equation (52) gives:

$$\frac{\overline{\Lambda}(t)}{\bar{e}(t)}.\xi.\frac{2\pi^2\rho_e^3(1-k)(1-k^2)}{ln(1/k)}.N = \frac{\mathrm{P}_{eff}}{2\pi\bar{\rho}.N} \tag{53}$$

This demonstrates that the mean shear factor $\overline{\Lambda}(t)$ varies in the same way as the mean gap clearance $\bar{e}(t)$. As one of the objectives is to find the expression of the normal reaction force exerted on the fibrous pads, one can derive it from (29) and (52):

$$F_n^{eff}(t) = \left(\frac{\overline{\Lambda}(t)}{\bar{e}(t)}.\xi.\frac{2\pi^2\rho_e^3(1-k)(1-k^2)}{ln(1/\mathrm{k})}.N\right)/f(t) \tag{54}$$

Replacing $\bar{\rho}$ by its expression (28) in Equation (37), the net power P_{eff} consumed during a refining trial can be derived:

$$\mathrm{P}_{eff} = \frac{8\pi^3\rho_e^4(1-k)(1-k^3)}{3.ln(1/k)}.\xi.\frac{N^2\overline{\Lambda}(t)}{\bar{e}(t)} \tag{55}$$

In the past, many authors have studied the refining process and Dalzell [31] as cited by Ebeling [23] wrote an empirical equation in 1961 as follows:

$$\mathrm{P}_{eff} = k_1\frac{\mu}{(\bar{e})^n}.D.L.\xi.V_P^2 \tag{56}$$

where μ, D, L and V_P stand for a coefficient of viscosity, an effective diameter, an effective length and the peripheral rotation speed. If the Dalzell equation is reworked and V_P is replaced by $2\pi\rho_e N$, one can obtain:

$$\mathrm{P}_{eff} = k_1'.4\pi^2.D.L.\rho_e^2.\frac{N^2.\mu}{(\bar{e})^n} \tag{57}$$

It is remarkable to have developed a fundamental theoretical description of the refining process involving the mean shear factor $\overline{\Lambda}$. This equation clearly provides the foundation of the previous empirical work undertaken by Banks [30], Dalzell [31], Leider and Nissan [34]. Equations (55) and (57) are analogous and Dalzell remarked that his "coefficient of viscosity μ" is strongly affected by the concentration: that is it increases with increasing concentration. In fact, μ is proportional to the mean shear factor $\overline{\Lambda}$ that generalizes the pulp apparent viscosity μ_a. The strong variation of μ_a with concentration has been found experimentally ([32] for example). If the net power and the mean gap clearance are recorded on a refiner, the mean shear factor $\overline{\Lambda}$ can be determined by the following during the refining process:

$$\overline{\Lambda}(t) = \frac{3.ln(1/k)}{8\pi^3(1-k)(1-k^3).\xi}.\frac{\mathrm{P}_{eff}.\bar{e}(t)}{\rho_e^4.N^2} \tag{58}$$

If the net power is eliminated from the previous equation using the friction coefficient expression, Equation (45), then a law similar to that of Petroff in lubrication theory may be obtained:

$$f(t) = \frac{2\pi.(1-k)}{ln(1/k)} \cdot \frac{\overline{\Lambda}(t).N}{(\overline{P_m}(t) - \overline{P_h})} \cdot \frac{\rho_e}{\bar{e}(t)} \tag{59}$$

The two last ratios play an important role in the theory of lubrication of bearings but in our case, all the key-parameters are related according to this analysis.

Experimental research

In order to understand the phenomena which occur in refining with the same fibrous raw material, a set of experimental trials was undertaken. For a long fibre pulp and various mixtures of this with a chemical-thermal-mechanical pulp, the normal compression force and the corresponding gap clearance were measured during refining trials performed in hydra-cycle mode on a single-disc refiner with radii $\rho_i = 66.5$ mm and $\rho_e = 152.5$ mm. At constant pulp consistency $c = 32$ kg/m^3, volumetric flow $Q = 9.6$ m^3/h, rotation speed 1550 rpm, cutting speed $\dot{L}_c = 11$ km/s and with the net power consumed varying from 6.3 to 11 kW, the effective specific energy was varied according to the time during a given trial:

$$E_{eff}(t) = \frac{P_{eff}.t}{m_s} \tag{60}$$

The corresponding specific edge load changed from 0.60 J/m to 1.00 J/m for the long fibre and from 0.29 to 0.50 J/m for the whole pulp. In the different trials, the bar width, the groove width, the net power applied and the mean crossing angle of the bars were all used as variables to acquire the results represented in Figure 14.

The difference between the calculated and the measured values was always found to be below 6%: an acceptable discrepancy for industrial data obtained on a pilot machine.

These results tend to validate the following model for the normal compression force versus the gap clearance when refining this raw material:

$$F_n(t) = \frac{F_n^{\infty}}{1 + \delta.\bar{e}(t)} \tag{61}$$

The numerator expresses the maximum normal force of compression when

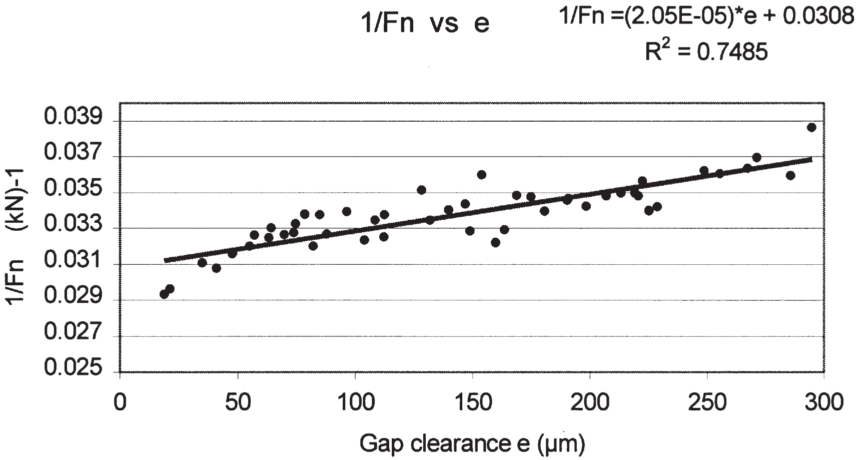

Figure 14 Inverse of the normal compression force vs. the gap clearance.

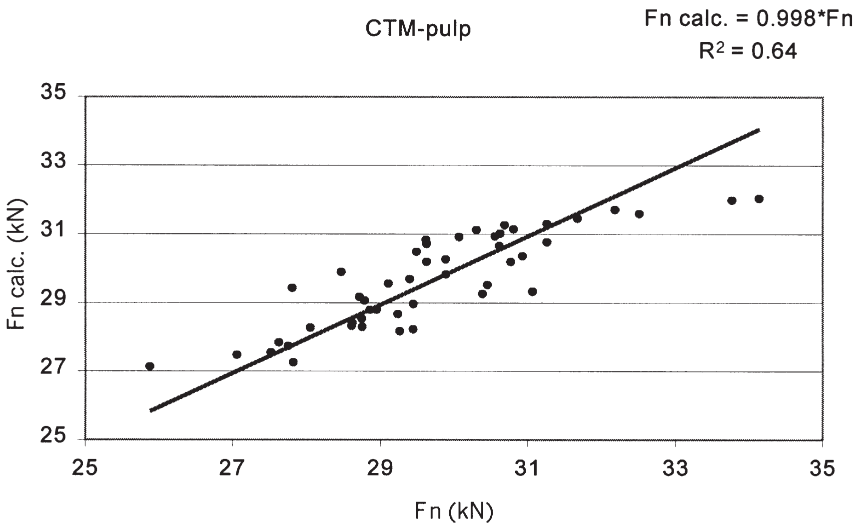

Figure 15 Comparison between the calculated and practical values.

the gap clearance is equal to zero. For example, on the CTM-pulp studied, this force was found in the range of 32.5 kN and δ was equal to 6.64 10^{-4} (μm^{-1}). Combining the theoretical expectations (33) with the practical findings, the effective normal force may be written as:

$$F_n^{eff}(t) = (F_n^{\infty} - F_n^{0}).\left[\frac{1 - \left(\dfrac{\delta.F_n^{0}}{F_n^{\infty} - F_n^{0}}\right).\bar{e}(t)}{1 + \delta.\bar{e}(t)}\right] \tag{62}$$

On the right-hand, the first term between parenthesis is the maximum effective normal force that can be applied to the fibrous pads compressed in the confined areas. This expression shows that a critical gap clearance is needed to develop a positive and effective normal force. What does that mean in practice? If the gap clearance is above this critical value, then no appreciable fibre refining effect will occur. This critical value mainly depends on two mechanical parameters which are the limiting values of the normal compression force when the gap clearance is high enough (F_n^{0}) and when it is equal to zero (F_n^{∞}). The last parameter (δ) expresses the changes in compressibility of the fibrous pads in the intercrossing areas of bars during the refining process. This critical gap clearance is given by the following equation deduced from the expression (62):

$$\bar{e}_c = \left(\frac{F_n^{\infty}}{F_n^{0}} - 1\right).\frac{1}{\delta} \tag{63}$$

Applied to the data for the CTM-pulp, a critical gap clearance of 285 µm was found. From the knowledge of the effective normal force, the global friction coefficient may be easily derived. When refining in hydra-cycle mode, this coefficient changes with time according to the variations in the mechanical properties of the metal bar/fibre suspension combination. This subject has for a long time been a matter of speculation. Using expression (62), this change can be calculated whenever the effective normal force is strictly positive:

$$f(t) = f_{min}.\left[\frac{1 + \delta.\bar{e}(t)}{1 - \dfrac{\bar{e}(t)}{\bar{e}_c}}\right] \tag{64}$$

where the minimum value of the global friction coefficient is given by the following expression:

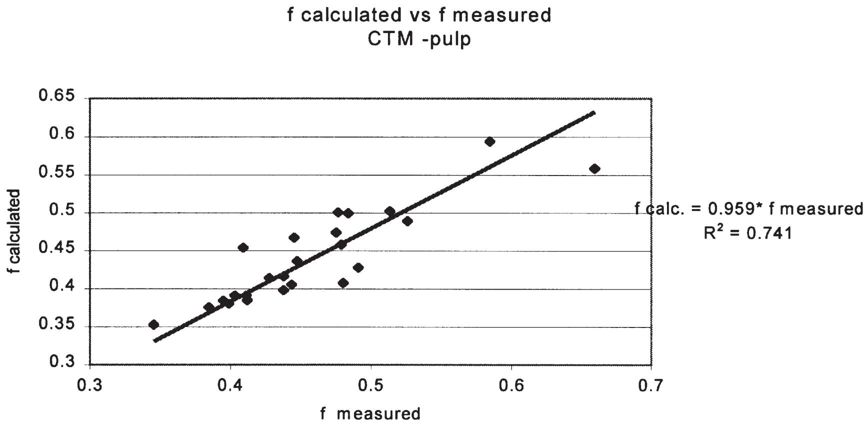

Figure 16 Validation of the model for the global friction coefficient for a CTM-pulp.

$$f_{min} = \frac{F_f^{eff}}{F_n^{\infty} - F_n^{0}} \tag{65}$$

During the refining process, the global friction coefficient decreases with the gap clearance following Equation (64). The proposed model was validated on the chemical-thermal-mechanical pulp with the previous data concerning the whole pulp, as exemplified in Figure 16. However, some limitations arise from this model, the friction coefficient can not be reasonably defined when we are approaching the critical gap clearance since the effective normal force reaches zero in that case.

Interpretation in terms of a pressing process

If the fibrous raw material is confined in the intercrossing areas of bars, the process may be interpreted in terms of consolidation (pressing). In the case of a solid-liquid porous medium, the overpressure $\overline{P_m} - \overline{P_h}$ can be written as a sum of two pressures:

$\overline{P_s}$: the structural pressure exerted on the solid phase (the fibres)
$\overline{\Delta P_h}$: the hydraulic pressure excess above its reference value $\overline{P_h}$.

Study of the pressing process [35] identifies two specific behaviours: compression controlled and flow controlled modes. In compression controlled mode, the pressure is entirely supported by the solid phase (the fibres). This occurs in refining when the gap clearance is decreasing and the fibre cutting effect reaches a maximum. Referring to the previous analysis, the effective normal force is thus at a maximum while the friction coefficient is minimal. This is a regime of mainly solid/solid friction phenomena. Then, another regime takes over when the normal force and friction coefficient are quasi-constant. In that case, an analogy with flow controlled pressing can be made. The overall mechanical pressure $\overline{P_m}$ is only in equilibrium with the hydraulic pressure $\overline{P_h} + \overline{\Delta P_h}$ and the effects are mainly due to solid/liquid friction. It is the perception of the author that the refining process may be understood by taking into account successively the two regimes: first the compression controlled; then the flow controlled. For some fibrous raw materials, the first regime may be very short-lived so that the friction force maintains a constant value given by the overall friction coefficient for the refining process.

Determination of a Sommerfeld number for disc refiners

In the hydrodynamic modeling of the refining process performed in a Valley beater [32] a dimensionless equation was proposed for the normal load exerted on the fibrous networks or pads in the gap clearance:

$$r_n = a + b.\left(\frac{\mu_a.U.R}{P_0.(\delta h)^2}\right) \tag{66}$$

where: μ_a is the pulp apparent viscosity, U is the peripheral speed of the cylinder, R is the radius of the cylinder, P_0 is the reference pressure in the grooves, δh is the vertical displacement of the cylinder that specifies the gap clearance. If Equations (33), (34) and (54) are combined, then the dimensionless normal load can be rewritten as follows:

$$\frac{F_n(t)}{F_n^{\,0}} = 1 + \frac{\xi.(1-k)}{ln(1/k)}.\left(\frac{\overline{\Lambda}(t).V_p}{f(t).\overline{P_h}.\bar{e}(t)}\right) \tag{67}$$

This suggests a Sommerfeld number since the expression between parenthesis above can be defined by analogy with a Valley beater. Hence, for a disc-refiner:

$$S_d(t) = \left(\frac{\overline{\Lambda}(t).V_p}{f(t).\overline{P_h}.\bar{e}(t)}\right) \tag{68}$$

One remark arises from the previous paragraphs. Performing refining trials with constant effective power keeps the ratio $\overline{\Lambda}(t)/\overline{e}(t)$ constant, see Equation (53). This means that the Sommerfeld number is inversely proportional to the friction coefficient. A simplified expression of the inverse of the friction coefficient may be written:

$$\frac{1}{f(t)} = \frac{\delta.F_n^0}{F_f^{eff}}.(\bar{e}_c - \bar{e}(t)) \tag{69}$$

Taking into account Equation (52) for the effective friction force together with Equation (69), a very simple formula is obtained in the case of a disc refiner which greatly simplifies the Sommerfeld number:

$$\frac{F_n(t)}{F_n^0} = 1 + \delta.(\bar{e}_c - \bar{e}(t)) \tag{70}$$

This formulation is valid when the gap clearance is less than or equal to some critical value at which refining effects begin to occur on the fibrous raw material.

According to this research, the global set of data must follow the predicted evolution given by Equation (70). The results presented on Figure 17 are as satisfactory as possible with industrial data.

The delta value is known and, from the interpretations of the experimental

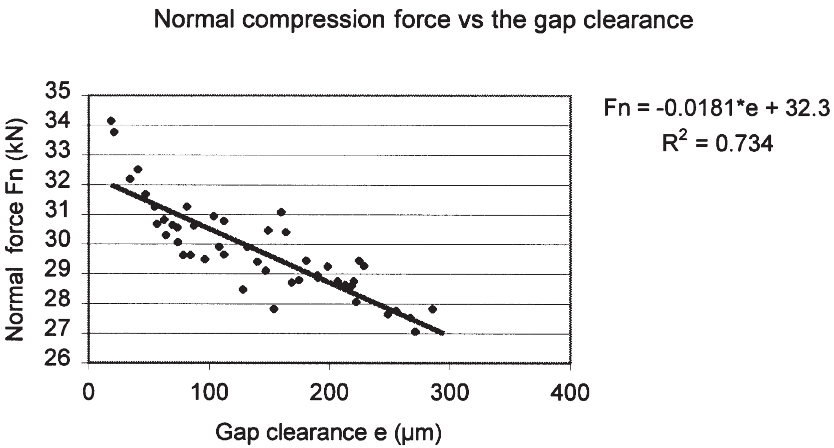

Figure 17 Variation of the normal compression force with gap clearance.

data, the critical gap clearance and the normal force in no-load conditions can be quantified. $F_n^0 = 27.2$ kN and $\overline{e}_c = 285\ \mu$m. Comparisons between both analysis lead to the following expression which linking the physical quantities to each other:

$$F_n^0.(1 + \delta.\bar{e}_c) = F_n^\infty \tag{71}$$

Consequently, it is then possible to analyze the refining process in terms of the changes of the average mechanical pressure. Given this and rewriting Equation (44) leads to:

$$\overline{P_m}(t) - \overline{P_h} = \frac{\overline{P_h}}{\xi}.\delta.\left(\bar{e}_c - \bar{e}(t)\right) \tag{72}$$

In the limiting case where the gap clearance is chosen at zero, the maximal mechanical pressure over the hydraulic reference is equal to: $(\overline{P_h}/\xi).\delta.\bar{e}_c$ or 0.35 MPa.

Thus, both the effective normal force and the effective average mechanical pressure vary linearly with the mean gap clearance, one of the key quantities in understanding the refining process.

Comparison with other mechanistic theories

Recently [38], an expression has been derived to predict the force acting on an ideal floc undergoing compression between the passing bars of a refiner. The model equation is based upon three assumptions about flocs: they are spherical in shape with fibres evenly spaced in any cross-section; they cannot support significant normal load until the majority of fibres are in contact; and they display linear elastic behaviour under compression.

Figure 18 demonstrates the existence of two regimes:

- in the first, under uniaxial compression in the y-direction, the authors assume the dominant action to be densification by decreasing pore size and increasing fibre contact. The diameter of the ideal floc changes from L_0 to $\gamma . L_0$
- in the second, at some degree of compression, the number of fibres in contact is such that further compression of the floc requires significant force to reduce the inter-fibre spacing. For wood fibres with hollow lumens, additional force is required to collapse the individual fibres themselves and to squeeze water out of the cell wall.

At the end of the first regime, the maximum floc size is:

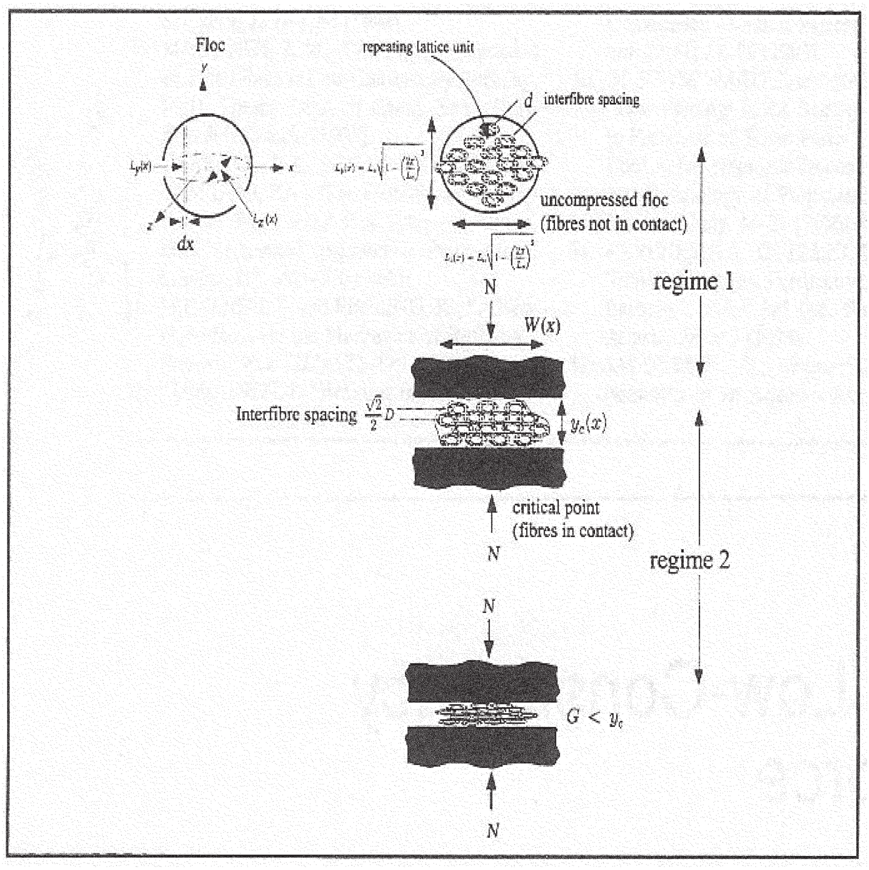

Figure 18 Schematic view of fibres in flocs undergoing compression [16].

$$y_c'(0) = \frac{\pi}{4.\gamma^2}.\frac{\rho_0.(a.D)^2}{\omega} \tag{73}$$

where D is the fibre diameter, a is the ratio of inter-fibre spacing to fibre diameter, ρ_0 the bulk fibre density of the floc and ω the fibre coarseness. As shown in [38], the maximum floc size was found to vary between 0.2 to 0.5 mm for a hardwood and a softwood pulp.

At the onset of the second regime, the effective normal force $F_n^{eff}(t)$ begins to increase significantly from zero. This may correspond to the critical gap clearance below which refining effects are supposed to occur. In this mechanistic theory [38], it is said that in compression tests performed on a laboratory apparatus with nylon flocs, the ratio of the gap clearance to the diameter of the uncompressed floc has to be lower than a critical value for any normal force to be measured. When this ratio is small enough, there is found to be a decreasing linear relation between normal force and gap clearance. In other words, as the gap clearance decreases with the refining process, the normal force increases.

All these observations, obtained with raw materials (textile fibres) different from cellulose fibres, are nevertheless consistent with the physical description of the refining process proposed in this paper. The authors of [38] believed that the general conclusions drawn in their mechanistic theory with nylon fibres would have applicability to the refining of chemical pulps. We can prove now that their expectations were correct.

Derivation of a refining intensity [7]

When studying the probability of occurrence of different refining effects on fibres, the notion of refining intensity distribution is used. This section proposes first to determine a refining intensity taking into account the mean number of inter-crossing areas described by the bars in their relative motion. Then, by calculating the ratio of the effective normal force (or tangential force) by the mean number of inter-crossing areas, it may be possible to calculate some average values of these elementary forces. This leads to the concept of reference specific edge load that accounts for the main engineering parameters. This reference specific edge load is a measure of the effective force applied, on average, at the inter-crossing area of bars.

We consider the case only of a single-disc refiner, though it can be generalised to other types of refiners. Let's begin with Figure 19, where the bars are parallel to each other in sectors. This geometry is very often met in the paper industry. A close examination of this figure indicates that the first full bar is located on the right side of the sector, we call this configuration LE. Hence, Figure 19 reflects a combination LE/LE for the rotor/stator pair. If the number of crossing areas on an elementary annulus is counted, it is:

$$\frac{2\pi\rho \;\, d\rho}{(a_s + b_s)(a_r + b_r)} \left| \sin\left(\varphi_s(\psi) + \varphi_r\right) \right|$$

It may be noticed that $\varphi_s + \varphi_r$ is the crossing angle $\gamma(\psi)$ of the bars. For the stator, Figure 19 clearly demonstrates that $\varphi_s(\psi)$ varies between β for the first full bar located on the right-side of the circumference of radius ρ and $\beta + \theta$ for the last bar located on the left-side of the sector. For the rotor, the angle φ_r

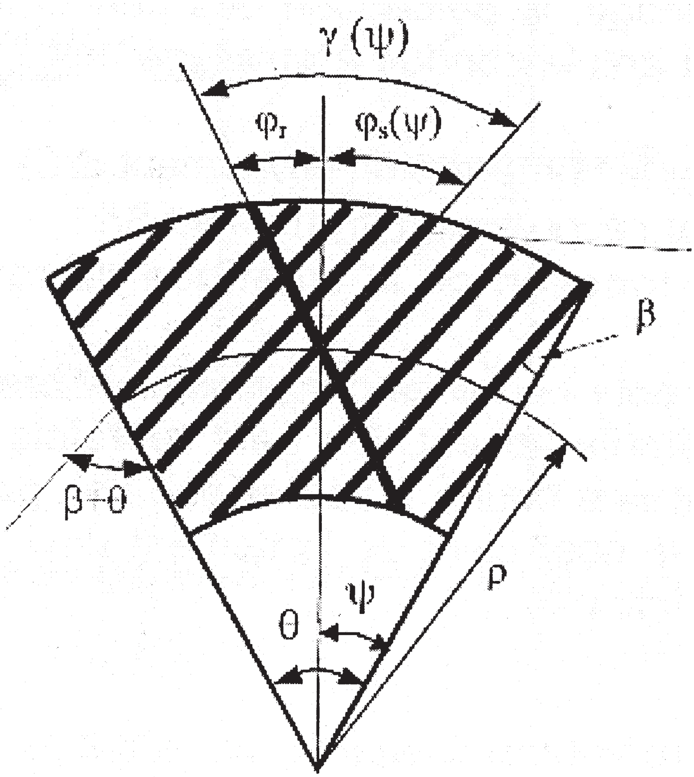

Figure 19 LE/LE sector configuration.

varies between α and $\alpha + \theta$. Hence, during relative motion, the number of inter-crossing areas varies between:

$$\frac{2\pi\rho d\rho}{(a_s + b_s)(a_r + b_r)} \sin(\alpha + \beta) \quad \text{and} \quad \frac{2\pi\rho d\rho}{(a_s + b_s)(a_r + b_r)} \sin(\alpha + \beta + 2\theta)$$

In the case when $(\alpha + \beta) > 0$, its average value may be calculated by a double-integration as follows:

$$\frac{2\pi\rho d\rho}{(a_s + b_s)(a_r + b_r)} \cdot \frac{1}{\theta^2} \int_{\alpha}^{\alpha+\theta} \int_{\beta}^{\beta+\theta} \sin(\varphi_s + \varphi_r) d\varphi_s d\varphi_r$$

The first integral gives:

$$\int_{\beta}^{\beta+\theta} \sin(\varphi_s + \varphi_r) d\varphi_s = \cos(\beta + \varphi_r) - \cos(\beta + \theta + \varphi_r) \qquad (74)$$

and the second one:

$$\int_{\alpha}^{\alpha+\theta} [\cos(\beta + \varphi_r) - \cos(\beta + \theta + \varphi_r)].d\varphi_r = 2\sin(\alpha + \beta + \theta) - \sin(\alpha + \beta) - \sin(\alpha + \beta + 2\theta) \qquad (75)$$

When these partial results are integrated over the complete annulus between the radii ρ_i and ρ_e, it is then possible to determine the mean number of crossing areas:

$$\bar{n} = \frac{\pi \rho_e^2 (1 - k^2)}{(a_s + b_s)(a_r + b_r)} \cdot \left[\frac{2\sin(\alpha + \beta + \theta) - \sin(\alpha + \beta) - \sin(\alpha + \beta + 2\theta)}{\theta^2} \right] \qquad (76)$$

With the help of some trigonometric calculations, the following equation is rewritten as:

$$\bar{n} = \frac{\pi \rho_e^2 (1 - k^2)}{(a_s + b_s)(a_r + b_r)} \cdot \left(\operatorname{sinc}\left(\frac{\theta}{2}\right)\right)^2 . \sin(\alpha + \beta + \theta) \qquad (77)$$

One way to understand this quantity is to consider an equivalent inter-crossing area, on average, which is equal to $(a_s + b_s)(a_r + b_r)/\sin(\gamma^*)$ with a new characteristic angle γ^* defined as follows:

$$\sin(\gamma^*) = \left(\operatorname{sinc}\left(\frac{\theta}{2}\right)\right)^2 . \sin(\alpha + \beta + \theta) \qquad (78)$$

This is the case when the facing surfaces have a LE/LE sector configuration (Figure 19). The calculations can be done in the same way when the configurations differ between the rotor sector and the stator sector.

Particular case of different configurations for rotor/stator sector

This situation may arise when the disc plates are not properly set in the refiner. Figure 20 illustrates this case. For example, if the rotor is installed in the LS-configuration while the stator is unchanged, we get a pair of sector (LS/LE) rather than (LE/LE).

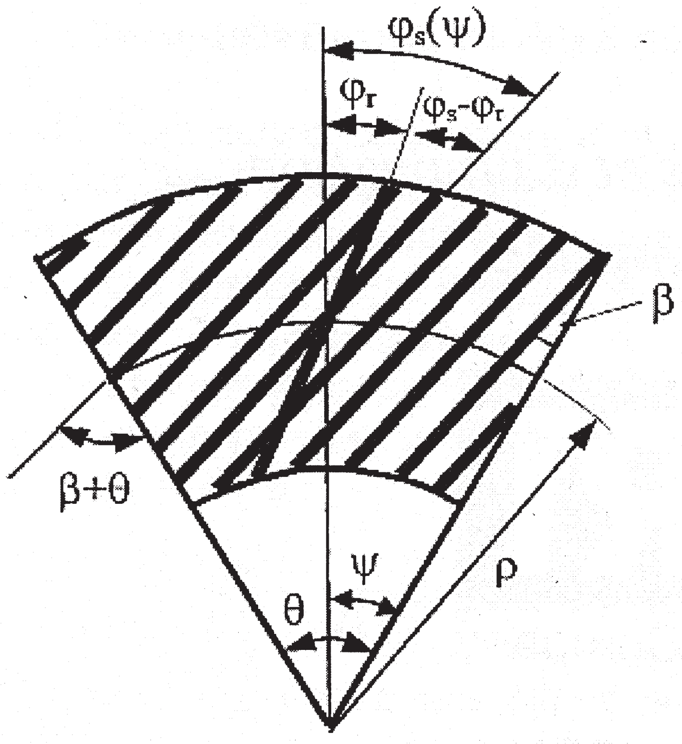

Figure20 Case of two opposite configurations.

The crossing angle becomes $|\varphi_s - \varphi_r|$ and the mean number of inter-crossing areas is given by the following expression:

$$\int_{\rho_i}^{\rho_e} \frac{2\pi\rho d\rho}{(a_s + b_s)(a_r + b_r)} \cdot \frac{1}{\theta^2} \int_{\alpha}^{\alpha+\theta} \int_{\beta}^{\beta+\theta} \sin(|\varphi_s - \varphi_r|) d\varphi_s d\varphi_r$$

In the case of two different angles α and β studied, and $\varphi_s > \varphi_r$, the first integral gives:

$$\int_{\beta}^{\beta+\theta} \sin(\varphi_s - \varphi_r)\,.\,d\varphi_s = \cos(\beta - \varphi_r) - \cos(\beta + \theta - \varphi_r) \tag{79}$$

and then:

$$\int_{a}^{a+\theta} \cos(\beta - \varphi_r) - \cos(\beta + \theta - \varphi_r).d\varphi_r = \sin(a - \beta + \theta) - 2\sin(a - \beta) + \sin(a - \beta - \theta) \quad (80)$$

To summarise at this point, a pair of sectors that only differs by their configurations leads to the following expression for the mean number of inter-crossing areas:

$$\bar{n} = \frac{\pi.\rho_e^2.(1-k^2)}{(a_s+b_s)(a_r+b_r)}.\left|\frac{\sin(a-\beta+\theta)+\sin(a-\beta-\theta)-2\sin(a-\beta)}{\theta^2}\right| \quad (81)$$

With the help of some trigonometric formulae, it is possible to rewrite the previous equation to give:

$$\bar{n} = \frac{\pi.\rho_e^2.(1-k^2)}{(a_s+b_s)(a_r+b_r)}.\left(\mathrm{sin}c\left(\frac{\theta}{2}\right)\right)^2.\sin(|a-\beta|) \quad (82)$$

By analogy with the case of two identical configurations, a characteristic angle may be defined γ^* by:

$$\sin(\gamma^*) = \left(\mathrm{sin}c\left(\frac{\theta}{2}\right)\right)^2.\sin|(a-\beta)| \quad (83)$$

PHYSICAL MEANING OF THE SPECIFIC EDGE LOAD

As indicated before and whatever the configuration of the facing plates, it may be interesting to calculate the ratio of the effective normal force by the mean number $\bar{n}$ of inter-crossing areas. This leads to the following equations:

$$\frac{F_n^{eff}}{\bar{n}} = \frac{P_{eff}}{f.2\pi.\bar{\rho}.\bar{n}.N} = \frac{1}{f.2\pi.\bar{\rho}}.\left[\frac{P_{eff}}{\bar{n}.N}\right] \quad (84)$$

Roux defined in 1988 [39], (by analogy with [40] and [41], themselves following the concepts proposed by Smith [42] in the beginning of the twentieth century), the term between brackets as the energy consumed per inter-crossing area. For example, on the same refiner, this term may be used to interpret the refining intensity when studying the shortening effect on fibres. However it is more desirable to continue the calculation by replacing the effective radius, see Equation (42).

$$\frac{F_n^{eff}}{\bar{n}} = \frac{3P_{eff}(1-k^2)}{f.4\pi\rho_e(1-k^3)\bar{n}.N} \quad (85)$$

If the substitution of the expression of the mean number of inter-crossing areas is performed, then the ratio becomes:

$$\frac{F_n^{eff}}{\bar{n}} = \left\{ \frac{3(a_s + b_s)(a_r + b_r)}{2\pi V_p.(1 - k^3)} . \frac{P_{eff}}{\rho_e^{\,2}} \right\} . \frac{1}{f.\sin(\gamma^*)} \tag{86}$$

where V_p is the peripheral tangential speed. In other work [43], the expression between parentheses was emphasised. It was defined as the reference specific edge load and noted C_s^0. The physical understanding of the reference specific edge load may be found in the derivation of an elementary effective force per inter-crossing area. The following equation has been extensively used in the practical refining trials performed on the disc-refiner pilot at EFPG (French Engineering School of Paper and Printing belonging to the Technological University INPG in Grenoble).

$$\frac{F_n^{eff}}{\bar{n}} = \frac{C_s^0}{f.\,\sin(\gamma^*)} \tag{87}$$

Even if average values are used in the calculations, the resulting expression still illustrates the de-coupling of the set of the following engineering parameters:

- internal radius,
- external radius,
- width of bars,
- width of grooves,
- peripheral speed,
- net power applied

compared to the set of geometrical parameters of the plates condensed in the characteristic angle that correctly accounts for the grinding angles and the relative configurations for rotor and stator plates.

On average, it may be interesting to determine the mechanical pressure above the hydraulic reference pressure, remembering Equation (29), which expresses the normal and effective compression forces. Combining with Equation (87), it gives [45]:

$$\overline{P_m} - \overline{P_h} = \frac{C_s^0}{f.\,a_s.\,a_r} \tag{88}$$

From this equation, we understand that the shortening effect on fibres may be attributed to the over-pressure on the fibrous pads in the confined areas described by the bar-crossings. All refining intensities defined by different authors are hence related more or less to the specific edge load concept.

Goncharov [37] earlier determined the physical nature of the specific edge load. If he considers two radial bars (for sake of simplicity) crossing each other, the specific edge load is defined as the work that the effective friction force dissipates during the crossing. In order to obtain the right units for the quantity under concern, the force per unit length of bars must be considered. If the friction coefficient is supposed to be constant and the variations of the effective normal force linear during the crossing, the following calculations can be done:

$$C_s^0 = \int_0^{a_s+a_r} f.\,[F_n(x) - F_n^{\,0}].dx = \tfrac{1}{2}.f.\,a_s.\,(a_s + a_r)\,.\,(\overline{P_m} - \overline{P_h}) \tag{89}$$

the special case where the width of stator bars, a_s, is equal to the width of rotor bars, a_r, leads to the formulation already given in (88) illustrating the coherence between the different interpretations proposed in this overview.

In fact, bars are not radial and make a certain angle with the radial direction. In a previous paragraph, an average crossing angle was defined as the characteristic angle γ^* (see Equations (78) and (83)). Let us begin with an identical configuration for the stator and rotor plates, for example the LE/LE configuration shown in Figure 19. In that case, the characteristic angle is not very different from the mean crossing angle $\bar{\gamma}$ of bars. If the friction coefficient together with the effective friction force are supposed to be constant during the crossing, then the following calculations may be performed recalling that the average bar angle is half of the mean crossing angle:

$$C_s = \int_0^{(a_r+a_r/2\,.\,\cos(\bar{\gamma}/2))} f.\,F_n^{eff}(x)\,.\,dx = f.\left\{\frac{1}{2}.(a_s + a_r)\,.\,\frac{1}{\cos(\bar{\gamma}/2)}\right\}.\,F_n^{eff} \tag{90}$$

The expression between brackets was defined by Lumiainen [45] as the impact length (IL), who defined the ratio of specific edge load to impact length as the specific surface load (SSL). This last concept is in fact the effective friction force per length of bars whose fundamental (not only empirical) importance is clear in this attempt to unify all the different approaches to understanding refining.

To summarize up to this point, the previous ratio may be a candidate for representing a refining intensity. It is not surprising that all attempts to define refining intensities mainly rely upon the well-known specific edge load. In fact, its unit itself is an indication of its physical nature: J/m means N, the unit of a force.

From the number of inter-crossings to the number of impacts

Because the refining process imposes a cyclic strain on fibres suggests that its action weakens the fibres by fatigue [46]. Therefore, the "type and degree of treatment" concept is an appropriate basis for describing refining action, as it characterizes the process by both the number of impacts and their intensity. This decomposition was first made in the early sixties by Lewis and Danforth [47], who defined both the number of impacts imparted to fibres by tackle elements (bar edges), and their severity. A large number of impacts of small intensity leads to fibrillation effects, whereas a small number of high intensity leads to shortening. The specific energy E_{eff} represents the combined effect of the intensity I_i and the number N_i of impacts. To be used, these concepts must be related to the engineering variables known to papermakers: the effective power P_{eff}, the fibre mass flux $\dot{M}$ through the refiner, and a *C_factor* as proposed by Kerekes [46]:

$$\begin{cases} E_{eff} = (C\_factor/\dot{M}) \,.\, (P_{eff}/C\_factor) \\ N_i = C\_factor/\dot{M} \end{cases} \qquad (91)$$
$$I_i = P_{eff}/C\_factor$$

In fact, in all theoretical approaches based on the concept of the specific edge load, the intensity refers to some form of cyclic deformation imposed on the fibre by bar crossings. One major difficulty lies in estimating the factor that transforms a bar crossing into an effective impact on fibres. Recently, Leider and Nissan [34], and Kerekes [46] have tried to calculate the probability that a bar crossing imparts an impact on fibres. In the *C_factor* analysis, the expression of the number of impacts per unit time on a fibre of length l on a circumference of radius ρ is given by:

$$\frac{dN_i}{dt} = \left[\frac{l}{l+c+e}\right] . \left[\frac{l}{2\,.\,\pi\,.\,\rho}\right] . n_1(\rho) \,.\, n_2(\rho) \,.\, \omega \qquad (92)$$

where l is the fibre length, c is the common height of stator and rotor bars, e is the gap clearance, ω is the rotational velocity of the refiner (in revolutions per second), $n_1(\rho)$,$n_2(\rho)$ are respectively the number of rotor bars and stator bars on the circumference of concern. The calculation of these numbers was proposed by Roux *et al*. [21]. For the case of an LE configuration for the sector shown in Figure 21:

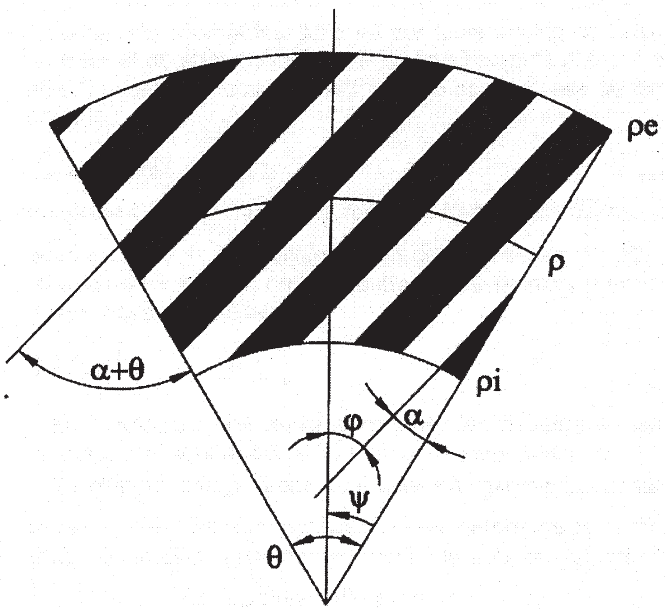

Figure 21 Rotor sector with LE configuration.

$$\begin{cases} n_1(\rho) = \dfrac{2\pi}{\theta} \cdot \dfrac{(\rho \,.\, \sin(\alpha + \theta) - \rho \,.\, \sin\alpha)}{(a_r + b_r)} \\[2ex] n_2(\rho) = \dfrac{2\pi}{\theta} \cdot \dfrac{(\rho \,.\, \sin(\beta + \theta) - \rho \,.\, \sin\beta)}{(a_s + b_s)} \end{cases} \tag{93}$$

Kerekes [46] introduced the relative density of the number of bars per unit arc length of stator and rotor separately, to homogenise the manipulated formula. If we follow the author as far as the differential analysis leading to the number of impacts on a fibre passing through the refiner, the following result is obtained in a rigorous way:

$$dN_i = \frac{4 \,.\, \pi^2 \,.\, l^2 \,.\, n_s \,.\, n_r \,.\, \omega \,.\, (e + n_s \,.\, b_s \,.\, c + n_r \,.\, b_r \,.\, c) \,.\, (1 + \tan(\alpha + \Psi_r) + \tan(\beta + \Psi_s)) \,.\, \rho^2 \,.\, d\rho}{Q \,.\, (l + c + e)} \tag{94}$$

Thus, after integration over the annulus for the case of a disc-refiner, the number of impacts per unit mass of pulp is written as follows:

$$N_{im} = \frac{4.\pi^2.l.\rho_w.C.n_s.n_r.\omega.c.(n_s.b_s + n_r.b_r).(1 + \tan(\alpha + \Psi_r) + \tan(\beta + \Psi_s)).(\rho_e^3 - \rho_i^3)}{3.\dot{M}.w.(l + c + e)} \tag{95}$$

where w is the fibre coarseness and ρ_w is the density of water. The angles $(\alpha + \Psi_r)$ and $(\beta + \Psi)$, which vary during the rotation, appear in the expression for the number of impacts on the fibres. Their average value is given by the integral:

$$\frac{1}{\theta^2}.\int_0^\theta \left(\int_0^\theta (1 + \tan(\alpha + \Psi_r) + \tan(\beta + \Psi_s)).d\Psi_s\right).d\Psi_r =$$

$$1 + \frac{1}{\theta}.ln\left[\left|\frac{\cos(\alpha)}{\cos(\alpha + \theta)}\right|.\left|\frac{\cos(\beta)}{\cos(\beta + \theta)}\right|\right] \tag{96}$$

In most refiners, the bar patterns on the rotor and the stator are similar (same bar width $(a_r = a_s = a)$, same groove width $(b_r = b_s = b)$, same bar height), while the gap clearance e is several orders of magnitude smaller than the bar height c. Making these justified assumptions, the *C_factor* can be shown to be given by:

$$C\_factor = \frac{4.\pi^2.\rho_w.C.\omega.(\rho_e^3 - \rho_i^3)}{3.w}.\left(\frac{l}{1 + l/c}\right).\left(\frac{b}{(a + b)^3}\right).F[\alpha,\beta,\theta] \tag{97}$$

where the last term is a function of the bar angle of the rotor α, of that of the stator β and of the sector angle θ. For example, in the case of the LE configuration shown in Figure 21, this function may be calculated by the following expression:

$$F[\alpha,\beta,\theta] = \frac{(\sin(\alpha + \theta) - \sin\alpha)^2(\sin(\beta + \theta) - \sin\beta) + (\sin(\alpha + \theta) - \sin\alpha)(\sin(\beta + \theta) - \sin\beta)^2}{\theta^3}$$

$$\bullet\left(1 + \frac{1}{\theta}.ln\left|\frac{\cos\alpha}{\cos(\alpha + \theta)}\right| + \frac{1}{\theta}.ln\left|\frac{\cos\beta}{\cos(\beta + \theta)}\right|\right) \tag{98}$$

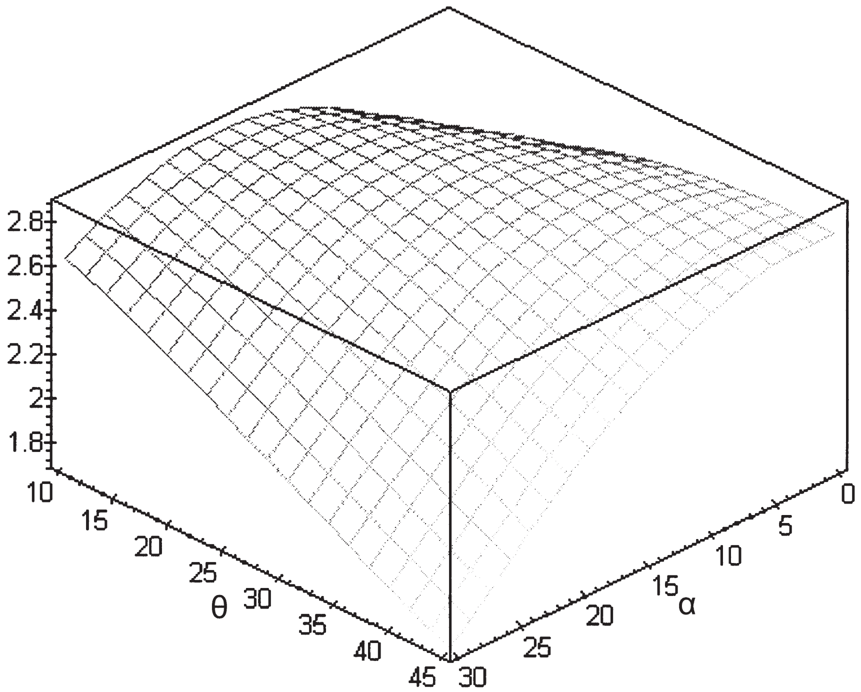

Figure 22 Variations of the angular factor F versus grinding angle $\alpha \in [0,30°]$ and sector angle $\theta \in [10,45°]$.

Equation (97) is of particular interest in studying the influence of different parameters on the number of impacts per unit mass of pulp; and, consequently, on the fibre shortening effects using the definition of the refining intensity (91). However, despite the rigour of the analysis used to derive the formula for the *C_factor*, it does not agree with experimental results when the angular parameters α,β,γ are varied.

Figure 22 illustrates how the angular factor F varies with the grinding and sector angles for the case of an LE/LE configuration and a common grinding angle for rotor and stator. From experimental results recently published [43], we know that increasing either of these angles leads to a decrease in the shortening effect on fibres (fibres are less cut), everything else being equal. This means that an increase in the number of impacts should be observed if the predictions are in accordance with the practical results. In fact, the predicted evolution of the angular factor is far more complex than the experimental observations. It does not agree when the sector angle is high, though it seems to be correct for small grinding angles.

However, predictions from changes in the other parameters in the expression for the *C_factor* indicate that the theoretical expectations for the variations of the number of impacts per unit mass of pulp are in accordance with the observed shortening effects on fibres.

Thus, it seems that this analysis represents a significant advance in understanding how to quantify the impact of a bar crossing on the fibres. Lastly, Croney and co-authors [48] proposed that the refining intensity may be adequately represented by the specific energy per impact, which means normalising the impact intensity by the product of the average fibre length and coarseness as follows:

$$S = \frac{I_i}{w.l} = \frac{P_{eff}}{(C\_factor).w.l} \tag{99}$$

From the refining intensity to its distribution

When studying the probability of occurrence of different refining effects on fibres, the distribution of refining intensity should be considered instead of its average value, as proposed by Giertz [28] and illustrated in Figure 23. It is

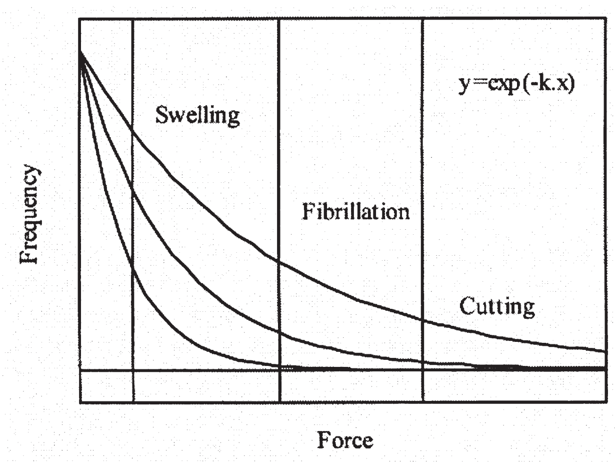

Figure 23 Distribution of impact intensity on fibres [28].

easy to demonstrate that the normalization of this distribution of impact intensity I on fibres leads to the following, where $<I>$ is the average intensity:

$$n^0(I) = \frac{exp(-I/<I>)}{<I>} \tag{100}$$

The collecting effects of the bars in industrial refiners have always been recognised, and sometimes observed [26] with high-speed cameras. In view of these observations, it seems reasonable to model the fibre breakage kinetics in industrial refiners as proposed in reference [49].

Among the results obtained is the dependence of the average fibre length on the specific energy E_{eff} when the reference specific edge load C_s^0 is chosen as the refining intensity:

$$\frac{l_f}{l_f^0} = \frac{1}{1 + \left[\frac{\mu_0 \, . \, E_{eff}}{2 \, . <I>} \, . \, exp\left(-\frac{I_{is}}{<I>}\right)\right]} \tag{101}$$

where μ_0 is the average fibre mass collected per unit active bar length in kg/m at the beginning of the refining process, and I_{is} is the yield refining intensity at which the fibrous materials break. Two observations can be made from this analysis:

- the shortening effect on fibres reaches an optimum when the average refining intensity $<I>$ used has the yield value I_{is}
- the ratio of this critical value to the average fibre mass effectively cut per unit active length gives an optimum specific energy for the refining effect under consideration.

The concept of optimum values for refining effects on fibres is a practical finding observed by Kerekes and co-authors [48]. Figure 24 illustrates the change in breaking length as a function of specific energy per impact (S) for different kinds of Kraft pulps, both hardwoods and softwoods. As remarked by Kerekes, the optimum value for S of 10 kJ/(kg.impact) seems independent of the fibrous materials analyzed in this study.

I complete this review of refining by emphasising how important is the finding that there is a single value for a fairly easily measured quantity which gives optimum refining effects for a wide range of fibre types.

Discovering the factors which determine this optimum value and how it varies for different refining effects must form the subjects for future research.

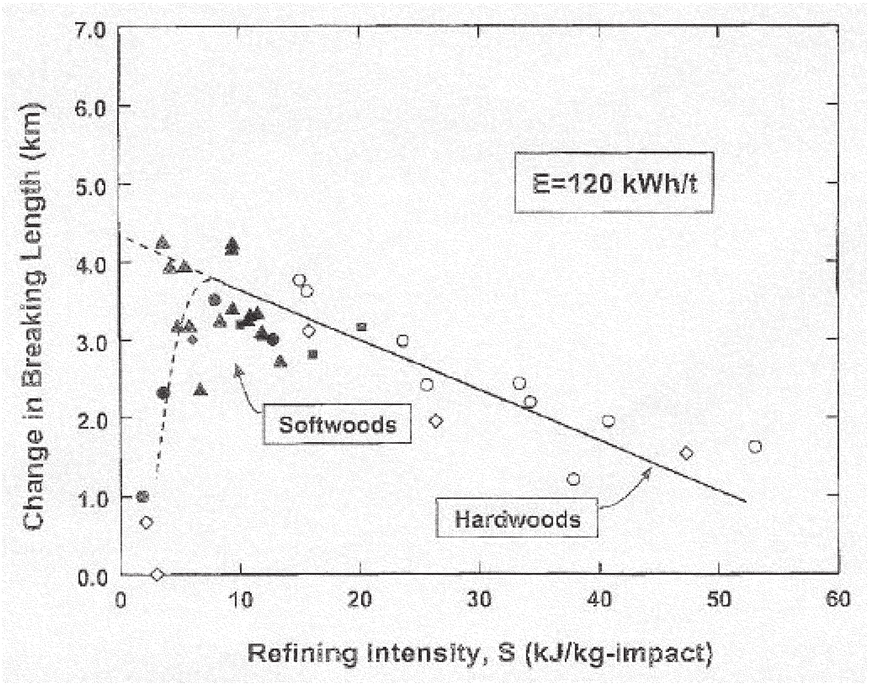

Figure 24 Change in breaking length as a function of the specific energy per impact.

The door is again wide open for research and investigations, both fundamental and practical.

HOT DISPERSING/MIXING

Dispersion and kneading

Introduction

This section mainly follows a paper [50] previously presented in the review Progress in Paper Recycling and published in Paper Recycling Challenge.

Early work on the dispersion of contaminants was begun in 1946 by a group of American papermills with the intent of recycling Kraft bitumen paper. It led to the development of a number of processes. The most common "thermal-mechanical" processes, or asphalt dispersion, consisted of high temperature (150°C) treatment in a device such as a disk type refiner [51,52].

The pressurized disk refiner processes have experienced considerable industrial development since the 1960s in contrast to the chemical or purely thermal processes [53] which have remained largely unused.

In mills recycling packaging papers and boards, hot dispersion is used to disperse thermofusible contaminants, such as waxes, hot melts and bitumen in order to avoid problems of spots (especially on hot plates during the converting of liners) and sticking between sheets. Dispersion and/or kneading equipment is found in most modern mills recycling packaging papers. It may be applied to the whole pulp or only to the long fibre fraction. However, in some applications, thanks to progress in fine slot screening technology, the use of hot dispersion is being questioned.

Hot dispersion in deinking plants has been utilized since 1978. Dispersion homogenizes the stock [54,55]; residual ink particles which have not been detached from the fibres (such as inks used for offset newspapers) are so finely dispersed as no longer to appear as undesirable specks. Dispersion or kneading has also been proposed to simultaneously disperse specks and as a high consistency mixer for bleaching the pulp [56]. Several papers proposing a hot dispersion stage between two flotation stages [57–59], or between a flotation stage and a washing stage [38] were presented during the 1989 EUCEPA Symposium in Ljubljana. Since the end of the 1980s, dispersion has become a basic treatment in multi-loop deinking processes. Dispersion and/or kneading is now included in all modern deinking facilities.

The main applications of dispersion and kneading are as follows:

- dispersion of hot melt contaminants, stickies, specks, residual ink,
- detachment of ink prior to deinking, or removal of residual ink prior to post-deinking,
- bleaching: thermal pretreatment, mixing chemicals or use as a bleaching reactor,
- microbiological decontamination: elevated temperatures in the presence of hydrogen peroxide destroy bacteria and fungi,
- changes in fibre properties: depending on device and operating conditions.

Principles of dispersion and kneading equipment

Hot dispersion consists of mechanical treatment performed generally at high temperature, high consistency and using appropriate techniques to transfer energy to the pulp.

Two main technologies exist: high speed dispersion and low speed dispersion, also called low speed kneading. Machinery suppliers, with a few rare exceptions, supply devices using one or the other technology. Consequently, these two technologies have often been contrasted. A few papers make comparisons of the two [61–64].

HIGH SPEED DISPERSION

High speed dispersion corresponds to a very short mechanical treatment (less than one second) applied to a small mass of fibrous material with a strong shearing effect due to a narrow disc gap and high rotational speeds. Speeds range from 1000–3000 rpm, but are generally 1200–1800 rpm. The dispersion effect results mainly from the impact of contaminants or ink against the tackle surface.

High speed dispersion (disc dispersers) has been developed by technology transfer from pulper-refiners for mechanical and thermal mechanical pulp (*Asplund-Defibrator*, *Beloit*, *Krima-Cellwood*, *Andritz-Sprout-Bauer, Kvaerner-Hymac, etc*.) with bar discs, and by the adaptation of high concentration deflakers with toothed discs (*Voith-Sulzer*, *Krima-Cellwood*). A disperser is illustrated in Figure 25.

The unit comprises stator and rotor disc. Stock is fed into the centre and due to centrifugal forces, the pulp moves radially and comes into contact with stator and rotor edges. Contacts with the rotor accelerate the pulp travel while contacts with the stator slows it down. These impacts induce a velocity differential resulting in shear forces and dispersion.

Some dispersers, (i.e., *Krima-Cellwood* or *Voith-Sulzer*) can be equipped with different types of teeth or bars; others are designed to operate at medium consistency (15%). The use of refiners operating at low consistency (5%) has also been proposed for the dispersion of specks [66].

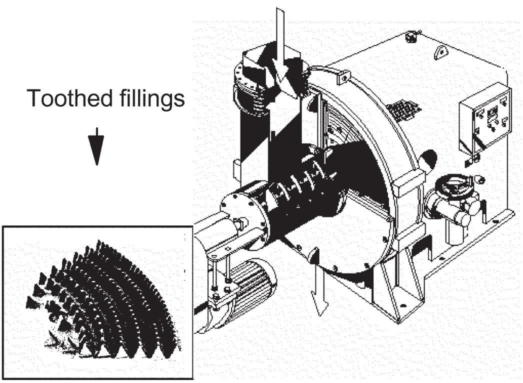

Figure 25 Disperser (Voith-Sulzer).

LOW SPEED KNEADING

Low speed kneading imparts a rather prolonged mechanical treatment (some minutes) to a large mass of fibrous material with a moderate shearing effect. This action is related to the relatively wide interbar clearance and slow rotation. Rotational speeds are normally 100–200 rpm, with a few exceptions at higher speed. The dispersion effect results mainly from fibre-to-fibre friction (rubbing action). In general, kneaders are devices in which the pulp is fed in by a screw and held by a discharge door as it is transferred under pressure between rows of fingers on a shaft and others on the stator wall.

Kneading technology for low speed dispersion consists of equipment with a single-shaft (*Erwepa, Voith*-*Sulzer*, *Lamort*-*Fiberprep*, *Maule*), or two shafts (*Shinhama, Modomekan*-*Ahlstrom*-*Kamyr*), specially developed for hot dispersion or resulting from technology transfer from stock mixers (*Micar Black*-*Clawson*). A typical single shaft kneader is illustrated in Figure 26.

Various designs are used for double shaft kneaders.

The *Shinhama* kneader, illustrated in Figure 27, has two counter-rotating shafts, one turning at 95 rpm, and the other rotating slightly faster at 110 rpm

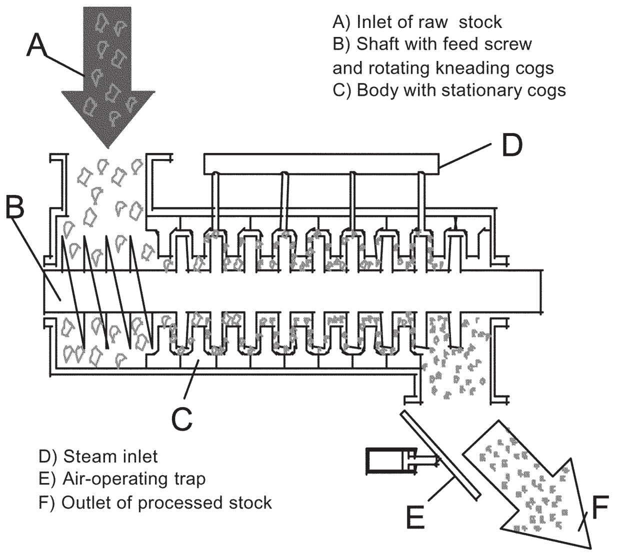

Figure 26 Single shaft kneader (Lamort).

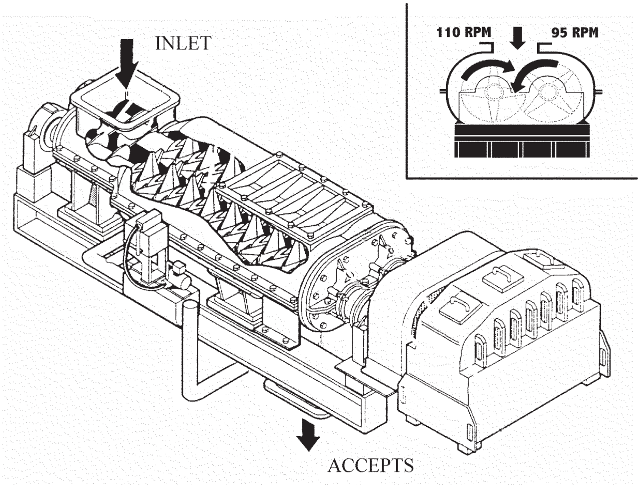

Figure 27 Double shaft kneader (Shinhama).

(i). The device previously called "Frotapulper" (*Modemekan-Kamyr*), and currently referred to as "MDR Kneader," (*Alhlstrom-Kamyr*) looks like a kneader, but the two screws counter-rotate synchronously at a speed of 900–1800 rpm (in the range of the of high speed dispersers). The device called "Micar" (*Black-Clawson*) runs at intermediate speed (400–500 rpm) [61].

The volume of pulp in the device is controlled by the discharge door. Stock moves through the device at a rather low speed. Differences in stock velocity are created inside the machine. The stock near the rotor is moving at a higher velocity than the stock near the stator wall. In the double shaft kneader, the rotors turn in opposite directions causing a shearing effect when the stock changes its direction of movement). These differences in velocity induce the fibre-to-fibre friction and the dispersion effect.

Operating conditions

The dispersion stage is implemented after a thickening stage. Various devices including the double wire thickener and screw press are used to concentrate the stock.

A heating screw can be implemented between the thickening stage and the dispersion unit. It is essential in high speed dispersion when steam is used to increase the pulp temperatures to the appropriate level. In low speed kneading, steam can be introduced at the kneader itself, and a heating screw is not generally required.

The dispersion consistency is generally 25–30%, with some devices operating at up to 35–40%. Depending upon the pulp characteristics, some devices are designed to operate at medium consistency.

The operating temperature depends on the requirements of the dispersion and varies over a wide range. Some kneaders are operated without any steam input for deinking applications. In such cases, the increase of temperature (up to 40–60°C) arises from mechanical energy dissipation. Most applications use steam to raise the dispersion temperature to approximately 90°C. Some low speed kneaders and high speed dispersers are designed as pressurized units which can operate at temperatures up to 150°C. These conditions used to be necessary in asphalt dispersion.

For both types, the energy consumption is in the range of 35–100 kWh/t, with typical industrial values in the range 60–80 kWh/t. Various techniques can be used to adjust the energy consumption depending on the device used. These approaches include adjusting the pressure on the discharge door, the gap between rotor and stator, the inlet consistency, etc.

In deinking plants, dispersion is often combined with bleaching. Bleaching chemicals can be introduced at the heating screw or at the inlet of the dispersion unit, which functions also as a mixer or bleaching reactor. Depending on the operating temperature and the device used, retention time may or may not be required after the dispersion unit.

Generally the pulp discharged from a kneader does not require dilution and bleaching is at the kneading consistency. The pulp can be discharged at operating consistency in some high speed dispersers but generally dilution is required for discharging from these machines. In this case storage for extended bleaching is not possible.

CONCLUSIONS

Re-pulping (disintegration), refining or beating and hot dispersion are typically pulp treatment processes and have been discussed in this part of the review of Stock Preparation. As the subject is so wide, it was not the intention of the author to be exhaustive. Emphasis was directed mainly on the process engineering aspects of the unit operations which do not often receive proper attention. Chemical and physical-chemical aspects are beyond the scope of this paper, as are pulp dilution, transport and storage.

It is believed that substantial benefits are available to the papermaker who correctly re-pulps and disintegrates his pulps, whether virgin or recycled.

Achieving the theoretical understanding on which to do this requires that the process must be defined as a triple operation where agitation by bulk motion, mixing and dispersion occur simultaneously. Then the physical description of the phenomena may be undertaken in order to model the kinetics. Modelling which concentrates on the total contact area between the solid and the rotor, allows us to understand the role of this parameter in a first-order kinetic process, for each fibrous raw material chosen. Generalisation is then possible if we take account of the wet tensile strength compared to the mechanical force applied.

However, as the consistency increases, the friction forces (solid/solid and solid/liquid) are not confined to the surroundings of the rotor, but are present also throughout the whole volume. To allow for this situation, another approach was followed, leading to a model for the kinetic constant in the first-order process as a function of the mass consistency and of the power dissipated per unit volume. This model justifies performing pulp disintegration in the medium consistency range. Based upon it, it becomes possible to classify the propensity of a pulp to be disintegrated and the sensitivity to the consistency; two parameters are hence needed.

Pulping or disintegration is a key operation for deinking in the case of all recycled pulps. A rheological analysis based upon the globalisation of all the friction forces leads to the shear-factor, from the generalisation of the apparent viscosity. Experimental trials performed in a planetary mixer equipped with both a flat beater and a hook impeller on old newsprint papers determined if ink fragmentation may result from mechanical action by bulk friction. It was also found that the shear-factor is dependent on the nature of the impeller and is an increasing function of the consistency. However, if one considers the total amount of energy consumed whatever the consistency and type of impeller, master curves are obtained which explain the disintegration effects, the brightness of the entire pulp and the speck contamination. It is also proved that the planetary mixer is more efficient than the helical pulper. In the range of consistencies between 8–20%, model tools now exist for the papermaker and for the machine manufacturer to assess the operation of pulp disintegration in terms of pulp quality (lower contamination), higher productivity and energy savings.

The refining/beating of pulps has always been one of the most fundamental operations in the pulp treatment processes. The physical and almost mechanical characteristics for the pulp and the future sheet of paper are obtained at this stage. Despite its importance, it is also one of the more difficult to understand and many contradictions are found in different reported studies.

The purpose here was to analyse the physical phenomena in a global view since it remains very difficult (even impossible?) to describe the micro-processes at the scale of the entities under concern: fibres or flocs.

For the case of a single disc refiner (which can easily be extended to include conical refiners), a physical description of the global forces was given in terms of the tangential friction force, normal force, and friction coefficient. From this theoretical analysis, some empirical results (e.g. Leider and Nissan, Banks, Dalzell) can be justified since some well-known expressions can be naturally and rigorously demonstrated.

The theory thus developed was then applied to reality in the form of an industrial disc-refiner. By changing the widths of the bars and grooves, the net power applied, the specific edge load, the mean crossing angle of the bars, the level of refining for the same fibrous raw material, a model was validated to analyse the normal force applied and the gap clearance. Two parameters arose from this model: the maximum normal force (when the gap clearance approaches zero); and a parameter related to the change of pulp compressibility under refining conditions. A combination of both theory and practice leads, for the first time, to the existence of a critical gap clearance under which the refining effects may occur on fibres. Interpretations in terms of pressing and in terms of lubrication are then proposed. From these, the refining kinetics may be interpreted in terms of the evolution of the global friction coefficient versus the gap clearance. At the beginning of the refining process, the physical phenomena are mainly solid/solid friction: the shortening effects on fibres reach their maximum and the friction coefficient decreases sharply. This regime then gives way to one where solid/liquid friction dominates, allowing the friction coefficient to reach a constant value. The first regime may last so short a time that it is not observed in practice.

One fundamental result is obtained: the normal compression force is a decreasing linear function of the mean gap clearance. It is the understanding of the author that specific measurements must be developed and performed in order to be able to answer the practical and theoretical problems that are raised by the refining operation. Comparisons made with other mechanistic theories support the results proposed here.

When refining effects are studied, the importance of the concept of refining intensity is often emphasised, but without any proper understanding of how it can be defined and what it means physically. To contribute to better understanding of this important concept, this paper built up from first principles expressions for the normal (frictional) force and the normal force divided by the average number of bar crossings. These provided the foundations on which to develop the concept of the reference specific edge load, which now becomes a theoretical concept rather than an empirical convenience. Some conclusions are also given regarding the specific surface load and the impact length.

When developing theories about refining, it is also difficult to transform bar crossings into impacts on fibres. The *C_factor* analysis can contribute to this, though there are some discrepancies where geometrical angle parameters (particularly grinding and sector angle) are concerned.

Finally, some considerations on the distribution of intensity are given, and references to recent literature discussing optimal values both for the intensity and for the specific energy are given.

Historically, dispersion at high temperature was used to disperse bitumen when recycling asphalt impregnated papers. More recently, it has become commonly used to disperse other contaminants such as wax and hot melt glues, especially in recycling old corrugated containers (OCC).

For white recycled grades, hot dispersion was found useful to disperse hot melt contaminants, and to improve the visual appearance of the final sheet by reducing residual ink and specks. However, because dispersion does not remove contaminants, but disperses them into the pulp, it can induce some detrimental effects such as deposits on the papermachine. As a consequence of the progress made in cleaning and screening efficiency, the value of hot dispersion is now being questioned.

The future of hot dispersion is mainly related to the improvement of deinking technology. Both high speed dispersers and low speed kneaders are proposed as ways of improving ink detachment, mainly before post-flotation. Various dispersing and kneading technologies are available and the choice of the most effective type is the subject of debate. The important role of dispersers as mixers and reactors for bleaching chemicals is also emphasised.

New applications, such as microbiological decontamination by using chemicals in a kneader, has also been proposed, and will probably be an important topic in the near future.

REFERENCES

Re-pulping/disintegration operation

1. de Choudens, C., Angelier, R., Combette, Ph., “Pâtes mécaniques de résineux, pâtes chimicomécaniques de feuillus. Nouveau procédé de fabrication”, *Revue ATIP*, **38**(8): 405–416, Septembre/Octobre (1984).
2. Kurdin, J.A., Bohn, W.L., “Mechanical pulping by extrusion”, *Tappi Pulping Conference*, proceedings: 265–274, San Francisco, November 12–14 (1984).
3. de Choudens, C., Angelier, R., “Bleached high yield pulps with the bivis process constituted of two bivis machines in line”, *Das Papier*, **43**(10A): 8–12 (1989).
4. de Choudens, C., Angelier, R., Devic, M., Kervennal, J., “Chemical-thermomechanical pulps at high level of brightness obtained by the bivis process associated with a sulfonation in reducing medium”, *Paperi ja Puu*, **72**(3): 248–252 (1990).

5. de Choudens, C., Angelier, R., Brochier, R., Labalette, F., “Manufacture of unbleached high yield pulps for packaging papers by the bivis process from fibre sorghum”, *1st European Seminar on Sorghum for Energy and Industry*, Toulouse, 1–3 April (1996).
6. de Choudens, C., Angelier, R., “The manufacture of bleached chemical pulps for printing grades from annual plants by the bivis process”, *International Conference on Sustainable Agriculture for Food, Energy, and Industry*, Braunschweig, June 27–28 (1997).
7. Roux, J.C., “How to characterise the operation of disintegration?”, *Paper Engineering Seminar*, Terrassa, Spain (1999).
8. Peel, J.D., “Stock preparation”: *Paper Science and Paper Manufacture*, Gary A. Smook (ed. ?): Angus Wilde Publications Inc., p. 99 (1999).
9. Barfod, H., “Modern integrated broke handling systems”, *Pulp and Paper Canada*, **87**(5): p. 74 (1986).
10. Lamort, P., Lamort de Gail, P., “Re-pulping of wet-strength paper and paperboard with medium consistency pulping”, *Papier Carton et Cellulose*, **29**(4): p. 60–61 (1980).
11. Paraskevas, S., “High consistency re-pulping benefits and drawbacks”, *Tappi Pulping Conference*, Houston: p. 139–143 (1983).
12. Holik, H., “Towards a better understanding of the defibreing process”, *Tappi Engineering Conference*, Chicago: p. 223–232 (1988).
13. Wagle, D.G., Lee, C.W., Brodkey, R.S., “Further comments on a visual study of pulp floc dispersion mechanisms”, *Tappi J.*, **71**(8): pp. 137–141 (1988).
14. Bennington, C.P.J., Smith, J.D., Sui, O.S. and Wang, M.H., “Characterization of re-pulper operation for newsprint deinking”, *Tappi Pulping Conference*, Montréal, 3: p. 1083–1095 (1998).
15. Amaral, M.E., Renaud, M., Roux, J.C., “Cinétique de désintégration des pâtes à papier: modélisation du phénomène”, *Revue ATIP*, **54**(3–4): pp. 76–84 (2000).
16. Fabry, B., “Etude de la rhéologie des suspensions fibreuses concentrées dans le but d’améliorer le recyclage des papiers”, *Thèse de Doctorat de l’INPG en Génie des Procédés*, Grenoble (1999).
17. Fabry, B., Roux, J.C., Carré, B., “Characterization of friction during pulping: an interesting tool to achieve good deinking”, *Journal of Pulp and Paper Science*, foreseen in autumn 2001.
18. Merrett, K.J., “Repulping at high consistencies”, *Appita*, **40**(3): pp. 185–188 (1987).
19. Savolainen, A., Jussila, T., Nikula, S., “Defibreing and specific energy consumption in bale pulpers”, *Tappi J.*, **71**(11): pp. 147–153 (1991).
20. Fabry, B., Roux, J.C., Carré, B., “Pulping, a key-factor for optimising deinking”, *Congrès de l’ATIP*, Bordeaux (2000).
21. Sousa-Santos, A., “Le rôle des tensio-actifs dans la flottation des encres off-set lors du désencrage des fibres cellulosiques”, *Thèse de Doctorat de l’INPG en Génie des Procédés*, Grenoble: 1997.
22. Metzner, A.B., Otto, R.E., “Agitation of Non-Newtonian fluids”, *Journal of American and Engineering Chemistry*, **43**(3): pp. 3–10 (1957).

Refining/beating

23. Ebeling, K., "A critical review of current theories for the refining of chemical pulps", *International Symposium on Fundamental Concepts of Refining*, Appleton: pp. 1–33 (1980).
24. Page, D.H., *The beating of chemical pulps – the action and the effects*, C.F. Baker and V.W. Punton (eds.): Mechanical Engineering Publications Limited: pp. 1–38 (1989).
25. Hietanen, S., Ebeling, K., "Fundamental aspects of the refining process", *Paperi ja Puu – Paper and Timber*, **72**(2): pp. 158–179 (1990).
26. Fox, T.S., Brodkey, R.S. and Nissan, A.H., "Inside a disk refiner", *Tappi J.*, **65**(7): pp. 80–83 (1982).
27. Steenberg, B., "Review of the effect of mechanical treatment of fibres", *Svensk Paperstidning*, **66**(22): pp. 933–939 (1963).
28. Giertz, H.W., "Ännu ett sätt att se pa° malningsprocessen", *Norsk Skogindustri*, **18**(7): pp. 239–248 (1964).
29. Roux, J.C., Chu, J.P., Joris, G., Caucal, G., "Théorie hydro-mécanique du fonctionnement d'un raffineur à basse concentration", *Revue ATIP*, **53**(4–5): pp. 106–116 (1999).
30. Banks, W.A., "Design considerations and engineering characteristics of disc refiners", *Paper Technology*, **8**(4): pp. 363–369 (1964).
31. Dalzell, D.R., "A comparison of paper mill refining equipment", *Tappi J.*, **44**(4): pp. 241–244 (1961).
32. Radoslavova, D., Roux, J.C., Silvy, J., *Hydrodynamic modelling of the behaviour of the pulp suspensions during beating and its application to optimising the refining process*, C.F. Baker (ed.): Pira International: pp. 607–639 (1997).
33. Roux, J.C., "La rhéologie pour mieux comprendre le fonctionnement des raffineurs en papeterie", *Les Cahiers de Rhéologie*, **17**(1): pp. 163–174 (2000).
34. Leider, P.J., Nissan, A.H., "Understanding the disk refiner – the mechanical treatment of the fibres", *Tappi*, **60**(10): pp. 85–89 (1977).
35. Wahlström, P.B., *Pulp and Paper Magazine of Canada*, **60**(8): pp. 379–401 (1960).
36. Caucal, G., Chaussy, D., Renaud, M., "Mesure des pulsations de pression en différents points d'un raffineur à disques", *Revue ATIP*, **46**(5): pp. 130–138 (1992).
37. Goncharov, V.N., "Force factors inside a disk refiner and its effect on the beating process" (translation), *Bumazh. Prom.*, (5): pp. 12–14 (1971).
38. Martinez, D.M., Batchelor, W.J., Kerekes, R.J., Ouellet, D., "Forces on fibres in low-consistency refining: Normal Force", *Journal of Pulp and Paper Science*, **23**(1): pp. 11–18 (1997).
39. Charuel, R., Roux, J.C., de Agostini F., Rousselle-Manuel, C., "Influence de la géométrie des lames sur le raffinage des pâtes chimiques", *Revue ATIP*, **42**(4): pp. 153–160 (1988).
40. Wultsch, F., Flucher, W., "The small Escher Wyss refiner as a standard testing instrument for modern stock preparation plant", *Das Papier*, **12**(13–14): pp. 334–342 (1958).

41. Brecht, W., Siewert, W., "Zür theoretisch-tecnisen Beurteilung des Mahlprozesses moderner Mahlmaschinen", *Das Papier*, **20**(1): pp. 4–14 (1966).
42. Smith, S., *The action of the beater*, Tech. Sect. Brit. Paper Makers's Assocn.: Great Britain and Ireland: 212 p: 1923.
43. Roux, J.C., Joris, G., Caucal, G., "Angular parameters beyond specific edge load", *The 6th Pira International Refining Conference*, Toronto (2001).
44. Roux, J.C., "Hydro-mechanical approach to understand the refining phenomena", *COST Meeting E7*, Technical University of Dresden: 25 May (1999).
45. Lumiainen, J., "A new approach to the critical factors affecting the refining intensity and refining result in low-consistency refining", *Tappi Papermakers Conference*, pp. 269–278 (1990).
46. Kerekes, R.J., "Characterisation of pulp refiners by a C-factor", *Nordic Pulp and Paper Research Journal*, 1 (1990).
47. Lewis, D.W., Danforth, J., "Stock preparation analysis", *Tappi J.*, **45**(3): pp. 185–192 (1962).
48. Croney, C, Ouellet, D., Kerekes, R.J., "Characterizing refining intensity for tensile strength development", 5th International Paper and Board Industry Conference, Scientific and Technical advances in refining, Vienna: 29–30th April (1999).
49. Roux, J.C., Mayade, T.L., "Modeling of the particle breakage kinetics in the wet mills for the paper industry", *Powder Technology*, 105: pp. 237–242 (1999).

Hot dispersing/mixing

50. Galland, G., Carré, C., Cochaux, A., Vernac, Y., Julien Saint-Amand, F., "Dispersion and Kneading", *Paper Recycling Challenge*.
51. Higgins, J.J., "Use of the asphalt dispersion system on waste paper", *Tappi*, **43**(1):132A-133A, January (1959).
52. Muir, J., "Processing of mixed waste paper", *Paper Technology*, **8**(3): 265–269 (1967).
53. Van Guelpen, L.C., "Dispersion of asphalt materials in paper stocks", *Tappi*, **43**(11): 162A-165A, November (1960).
54. Ortner, H., "Dispersion as a means of quality improvement of de-inked stock", *Paper Technology and Industry*, **19**(5): 143–147, May-June (1978).
55. Lamort de Gail, B. and Hétier, F., "Use of hot-dispersion system in treatment of secondary fibres", *Paper Technology and Industry*, **19**(2): 48–56, February (1978).
56. Cropper, M.A., "Advances in deinking and its use in improving quality of newsprint", *Tappi Paper Makers Conference*, 93–96, Atlanta, 26–29 April, (1976).
57. Ortner, H. and Fisher, S. , "Der Einsatz der Dispergierung zur Qualitätsverbesserung von deinkten Stoffen", *EUCEPA Symposium*, Ljubljana 23–27 October, (1989), Book of papers, V.II: 419–452 *also see Wochenblatt für Papierfabrikation*, **117**(19): 855–862, October (1989).
58. Linck, E., Matzke W. and Siewert W., "Systemüberlegungen beim Deinking von Altpapier", *EUCEPA Symposium*, Ljubljana (23–27 October 1989), Book of

papers, V.II: 361–378 *also see Wochenblatt für Papierfabrikation*, **118**(6): 227–232 (March 1990).
59. Johansson, O. and Steffner, S. , “Field Experience Gained in the New Deinking Plant at Hylte Bruks AB”, *EUCEPA Symposium*, Ljubljana, 23–27 October (1989).
60. Galland, G., Vernac, Y., Bernard, E. and Alibaux, P., “Amélioration de la blancheur des pâtes désencrées”, *EUCEPA Symposium*, Ljubljana (23–27 October 1989), *also see* revue ATIP **44**(3): 149–158 (March 1990).
61. McBride, D., “High-Density Kneading: an Alternative to Dispersion”, *1993 Tappi Recycling Symposium*, Notes: 173–180. New Orleans (28 February–4 March 1993).
62. McCarthy, C.E., “Dispersion and kneading”, *Tappi Deinking Short Course*, Houston, Wyndham Greenspoint Hotel, 10–12 June (1996).
63. McKinney, R. and Roberts, M., “Curl in recycled fibre: the impact of dispersion and kneading”, *Paper Recycling ’96 Conference*, Lancaster Hotel, London, 13–14 November (1996).
64. Cochaux, A., Carré, B., Vernac, Y. and Galland, G., “What is the difference between dispersion and kneading?”, *Progress in Paper Recycling*, **6**(4): 89–101, August (1997).
65. Sferrazza, M., Floccia, L., Favier, P. and Rihs, J., “Dispersion without dewatering: an innovative new approach”, *Paper Recycling ’96 Conference*, Lancaster Hotel, London, 13–14 November (1996).

Transcription of Discussion

STOCK PREPARATION PART 1 – PULP TREATMENT PROCESSES

Jean-Claude Roux

Ecole Française de Papeterie et des Industries Graphiques

Joint Comment submitted by J-C. Roux and R.J. Kerekes

This note is to clarify a statement concerning the C Factor on page 65 of this paper: ". . . .despite the rigour of the analysis used to derive the formula for the C factor, it does not agree with experimental results when the angular parameters . . . are varied."
" . . . increasing these angles leads to a decrease in the shortening effect . . . this means that an increase in the number of impacts should be observed. . ."

The C-Factor in fact correctly predicts this trend. For angles in the practical range, up to 52 degrees (combined angle), it predicts the number of bar crossings to increase with angle, and therefore intensity to decrease. This leads to a decrease in fibre shortening. The theory further predicts that the number of bar crossings reaches a maximum at about this angle. Beyond this value, the number of bar crossings decreases. In the limit of 180 degrees combined angle, it reaches zero. In this case the bars are concentric rings on the refiner plate, and therefore cannot create any bar crossings at all.

Kari Ebeling UPM-Kymmene Corporation

Could you please comment on the refining part of your presentation? How does the critical gap depend on the flocculation state? There has been photographic research done which shows that in the beginning of the refining bars are treating flocs – not individual fibres?

Jean-Claude Roux

I understand your question. In fact you saw that we decided to globalise the phenomena so I can come back to Figure 17 which expresses the forces or the inverse of the normal forces versus the gap clearance. You can see that in this curve there is one delta parameter that is proportional to the slope of this curve. We have not exactly the same behaviour for softwood or hardwood; I showed this CTMP pulp because we have plenty of results on this kind of pulp, but we also made interpretation on all kinds of fibrous raw materials. I mean the delta parameter is typically for raw material and it expresses some kind of compressibility the fibre pads in the inter-crossing zones, but it is a global view, you are right it depends on the state of flocculation. I know that there is some work on this subject to decided what is a consistency of the pulp pad or of the entities because you know it is a matter of speculation. Prof. Duffy, my colleague, put a classification of five types of flocs and probably ten types of flocs; what is a floc, it is a question probably that has been raised many times, but that is the reason why it is impossible for me to decide what is a kind of entity, and what is a type of floc. We measure only the delta which expresses the compressibility of the entities in the entire crossing zones. And this delta value is of course depending on the fibrous raw material.

Chad Bennington University of British Columbia and Paprican

I have one comment. You refer to work I have done to develop a model for deflaking, show a figure (Figure 3, Volume 1, Page 25) that summarizes some of my data, and discuss generating a master curve. If you take into account the wet-tensile strength of the paper and the maximum force generated by the rotor, you can collapse all these individual curves into one master curve. We are then in the same situation as you are, with a master curve that can predict the extent of paper deflaking. The shear-factor approach you have developed using Metzner and Otto averages out the shear rate in the vessel. Our model considers the maximum force generated at the rotor-suspension interface which is related to a characteristic shear rate in the vessel. I still think it is unclear whether deflaking is due to the application of this maximum force, or to a bulk shear rate. Both methods are actually related.

Jean-Claude Roux

Yes you are right, we can obtain some master curves if we take into account the wet tensile strength for different raw materials, and I know also that if we increase the consistency we have the inter-friction of fibre which is of importance and in your model you have put it in the maximum force, and also the effects are maximum around the volume of the rotor, and so I know that, but in your model you have one kind of rotor and what I have shown after that it is possible to integrate in a first order kinetic process also all the types of rotor by modelling the first order rate by the same expression which I was very surprised by this result, but I have to mention that it is true also for some small laboratory mixer, big pulper of any kind of size, according to me what is the one relevant parameter is the accumulated energy consumed per volume of pulp suspension.